



Measurement report: Simultaneous multi-site observations of VOCs in Shanghai, East China: characteristics, sources and secondary formation potentials

Yu Han¹, Tao Wang¹, Rui Li¹, Hongbo Fu*^{1, 2, 3}, Yusen Duan⁴, Song Gao^{4, 5}, Liwu Zhang¹, Jianmin Chen^{1, 2}

¹Shanghai Key Laboratory of Atmospheric Particle Pollution and Prevention, Department of Environmental Science & Engineering, Fudan University, Shanghai, 200433, P.R. China; ²Institute of Eco-Chongming (SIEC), 20 Cuinia Road, Chenjia Town, Chongming District, Shanghai 202162, China; ³Collaborative Innovation Center of Atmospheric Environment and Equipment Technology (CICAET), Nanjing University of Information Science and Technology, Nanjing 210044, P.R. China; ⁴Shanghai Environmental Monitoring Center, National Environmental Protection Shanghai Dianshan Lake Science Observatory Research Station, Shanghai, 200235, China; ⁵School of Environmental and Chemical Engineering, Shanghai University, Shanghai, 200444, China

Correspondence to: Hongbo Fu (fuhb@fudan.edu.cn)

Abstract. Volatile organic compounds (VOCs) have important impacts on air quality, climate, and human health. In order to identify the characteristics, sources and secondary formation potentials of the atmospheric VOCs varying with land use types, a concurrent multi-site observation campaign was performed at the supersites of Shanghai, East China, in the first three months of 2019. During the observation period, the average VOC concentrations were 21.39, 21.36 and 11.93 ppb at the Jinshan (JS), Pudong (PD) and Qingpu (QP) sites, respectively. The predominant VOC category was alkanes (49-61 %), followed by aromatics (11-21 %), alkenes (10-15 %) and alkyne (8-14 %) at the above sites. The sampling sites exhibited distinct diurnal variations and “weekend effects” of VOCs. The VOC concentrations increased by 27.15, 32.85 and 22.42 % during the haze events relative to the clean days during the measurements. Vehicle exhaust was determined as the predominant VOC source. The second largest VOC contributor was identified as industrial production at the JS and PD sites, while fuel evaporation was the second important source at the QP site. High potential source contribution function (PSCF) values appeared in the northeastern and northern Shanghai near the sampling sites, suggesting the strong local emissions. The secondary organic aerosol formation potential, mainly contributed by the aromatics, was higher at the JS site (1.00 $\mu\text{g m}^{-3}$) than those at the PD (0.46 $\mu\text{g m}^{-3}$) and QP (0.41 $\mu\text{g m}^{-3}$) sites. The VOCs-PM_{2.5} sensitivity analysis showed that the VOCs at the QP site could be more sensitive to the PM_{2.5} concentration relative to the other two sites. The ozone formation potentials (OFP) were calculated to be 50.89, 33.94 and 24.26 ppb during the campaign at the JS, PD and QP sites, respectively. The VOCs-O₃ sensitivity indicated that the VOCs-SO₃ values varied at the different sites and were primarily controlled by the alkene-related reactions. Alkenes and aromatics are thus the key concerns in controlling the VOC-related pollution of SOA and O₃ in the diverse districts of Shanghai. The findings of this study provide new insights into the accurate air-quality control at a city level in China due to a wide variety of land-use types. The results shown herein highlight that the simultaneous multiple-site measurements in the megacity or city cluster could be more appropriate to fully



understand the VOC characteristics relative to a single-site measurement performed normally.

35 1. Introduction

Serious air pollution in China is currently characterized by high level of ozone (O_3) and heavy loading of fine particulate matters (PM), both of which formation are greatly contributed by the atmospheric volatile organic compounds (VOCs) (Carter, 1994; Liu et al., 2008; Yuan et al., 2013; Lu et al., 2018; Ma et al., 2019; Yu et al., 2021). Atmospheric VOCs function as an important precursor of $PM_{2.5}$ (PM with an aerodynamic diameter less than $2.5 \mu m$), contributed greatly to the haze formation. In brief, the primary VOCs can be oxidized by $HO\cdot$, $RO_2\cdot$ and O_3 to produce secondary VOCs, which further transforms into SOA *via* a series of atmospheric processes (Odum et al., 1997; Ng et al., 2007; Heald et al., 2020). The secondary particles have strong influences on the atmospheric radiative forcing and climate (Sadeghi et al., 2021). On the other hand, VOCs reacts with NO_x and radicals *via* an array of photochemical processes to produce O_3 . Photochemical Assessment Monitoring Stations (PAMS) have confirmed 57 precursors of O_3 , including C_2 - C_{10} alkanes, alkenes, alkynes and aromatics (US EPA, 1990). Atmospheric O_3 has profound impact on the atmospheric oxidizing capacity, and has been widely proved to affect agriculture production and ecological conditions (Liu, 1987; Carter, 1994; Mousavinezhad et al., 2021; Sadeghi et al., 2021). Additionally, VOCs, along with derived secondary compounds, can damage human health and lead to many diseases such as cancers, respiratory and nervous system symptoms (Rumchev et al., 2007; Amor-Carro et al., 2020). Therefore, the VOC-related studies provide scientific-based information for the decision-makers who draw up strategies to control $PM_{2.5}$ and O_3 .

The temporal and spatial variations of VOC characteristics have been widely studied. In terms of seasonal variations, previous reports showed that colder seasons presented higher VOC levels than the ones at the warm seasons (Kumar et al., 2018; Sun et al., 2020; Debevec et al., 2021). For instance, Sun et al. (2020) found that the VOC pollution in the wintertime of Xi'an, China, was almost twice heavier than that in the summer. Such phenomenon could be mainly attributed to the fact that the higher emissions from anthropogenic sources including combustion and paint solvents occurred during the winter than those in the summer (Li et al., 2020). Furthermore, weaker atmospheric stability accelerates dilution and convection of the pollutants during the summer time (Monod et al., 2001; Dumanoglu et al., 2014). Besides, the elevated solar radiation and temperature during the summer were also responsible for the rapid VOCs loss through photochemical reactions (Lai et al., 2013; Kumar et al., 2018). The evolution of VOC concentrations from the clean days to haze events were also widely concerned. The occurrence of haze pollution was always accompanied by the rapidly increased VOC concentrations. For instance, in the Chinese cities, including Beijing (Wu et al., 2016); Shanghai (Han et al., 2017; Liu et al., 2021) and Wuhan (Hui et al., 2019), the VOC concentrations during haze pollution were 2-5 times higher than those in the clean days, which could be attributed to the stagnation condition hindering the vertical and horizontal dispersion of the VOC pollutants. In terms of spatial variations, urban and suburban areas normally suffer from heavier VOC pollution, relative to rural areas (Li et al., 2015a; Shao et al., 2016; Wang et al., 2016; Zhu et al., 2016; An et al., 2017; Zhang et al., 2017; Zhu et al., 2018; He et



al., 2019). Mozaffar et al. (2020) reviewed the VOC characteristics in the 35 worldwide cities, and illustrated that the VOC concentrations were generally higher at urban and suburban sites than those at rural sites. Moreover, comparing with the VOC pollution in the international areas including Tokyo (Hoshi et al., 2008), London (Schneidemesser et al., 2010), Los Angeles (Warneke et al., 2012), India (Kumar et al., 2018) and Houston (Sadeghi et al., 2021), Chinese cities are suffering from heavier VOC pollution. Although the VOC concentrations of China have decreased in the recent years along with the effective control strategies (Li et al., 2019b; Mozaffar et al., 2020), China is also an important VOC source compared with other countries on a worldwide scale.

VOCs are emitted primarily from biogenic and anthropogenic processes. The biogenic emissions (mainly from vegetations and trees) are responsible for approximately 1150 Tg carbon of the global VOCs per year. (Guenther et al., 1995; Atkinson and Arey, 2003; Calafapietra et al., 2009; Song et al., 2021). Chen et al. (2019) pointed out that biological emission dominated the North American VOC budget *via* the high-resolution chemical transport model. Despite the biological contributions, anthropogenic sources stand out to be an important VOCs contributor, especially in the megacities (Schwantes et al., 2016; Ahmad et al., 2017). Anthropogenic emission comprises vehicle exhaust, industrial pollution, painting solvent usage, fuel combustion, liquefied petroleum gas (LPG) usage and coal and biomass burning. The VOC sources varied with sampling locations, and the vehicle exhaust therein was proved by a plenty of studies to be the predominate VOC sources. For instance, vehicle-related sources explained 27 % of the VOCs in Tianjin, China (Han et al., 2011); 34 % in Zhengzhou, China (Nan et al., 2015); 34 % in central Shanghai, China (Cai et al., 2010a), and 24 % in Hawthorne, USA (Brown et al., 2007). Conversely, Zhang et al. (2018) claimed that industrial emission was a considerable source near an industrial site of Shanghai, China, accounting for more than half of the total VOC sources. In addition, LPG usage was discovered to exceed vehicle exhaust in influencing the VOC concentrations in Hong Kong (Lam et al., 2013). Although the recent emission inventory reveals the increasing contributions from solvent usage and industrial sources, traffic transportation is still highly responsible for the severe VOC pollution events (Liu et al., 2020, Li et al., 2019a; Song et al., 2021).

VOCs plays an important role in many atmospheric secondary processes, e.g. the formation of SOA and O₃. It has been widely reported that atmospheric VOCs has profound impacts on the concentration, physical property and chemical composition of SOA (Huang et al., 2015; Yuan et al., 2013), which acts as a significant component of PM_{2.5} (Huang et al., 2014; Zou et al., 2017). Firstly, in the presence of NO_x, the VOCs undergoes an array of photochemical processes to form secondary VOCs. The produced secondary VOCs further undergoes oxidation to generate multi-function-group species that declines the vapor pressure reduction (Seinfeld et al., 2001; Dechapanya et al., 2003a, b; Sjostedt et al., 2011). The intermediate compounds can undergo heterogeneous absorption on the pPM surface *via* gas-particulate partition with a moderate degree of decomposition and a significantly decreased in the vapor pressure, or through homogeneous reactions to transform into SOA (Pankow, 1994; Seinfeld et al., 2001; Yang et al., 2015; Han et al., 2017). Moreover, the O₃ formation potential of VOCs has attracted worldwide concern. Influenced by the complex atmospheric processes, the mechanism of O₃ formation can be classified into the NO_x-sensitive, transition and VOC-sensitive regimes. The NO_x-sensitive regimes of China are mainly distributed at the North, Northeast and Central China, part of Sichuan Basin (SCB) and mountainous area



100 with strong emissions of industrial, vehicular, power and biogenic (Wang et al., 2019a). In North, Central and East China, the
formation of O₃ is dependent of the NO_x transition regime. By contrast, VOC-sensitive regime does not have the regional
distribution as broad as the NO_x control area. The VOC-sensitive regimes are mainly located at the megacities in the Yangtze
River delta (YRD), Pearl River delta (PRD) and Beijing-Tianjin-Hebei (BTH) regions (Zhang et al., 2007; Xue et al., 2014;
Wang et al., 2019b). The VOCs transition area distributed at the urban area is mostly near the VOCs control regime. In detail,
105 atmospheric VOCs undergoes degradation to produce oxidants (HO₂ and RO₂), which further oxidize atmospheric NO,
followed by the production of NO₂ and finally the formation of O₃ through varied photochemical reactions (Wang et al.,
2017). Therefore, it is highly desirable to discuss the relationship of VOCs together with PM_{2.5} and O₃. The relevant results
would provide insight into the question of how VOCs are likely to response to the pollution of PM_{2.5} and O₃.

The atmospheric VOC characteristics have been widely discussed by single-site measurement in the worldwide cities. The
110 different research results can be explained by the varied emission sources and meteorological situations. However, limited
knowledge is available on the multi-site research at a city level, thus making the influences of different land use types on the
pollution VOC characteristics remain unclear. The previous multi-site measurements were performed at a regional scale
including Pearl River Delta region, China (Tang et al., 2008; Zhang et al., 2013); Xi'an, China (Song et al., 2021); VIR
region, Chile (Toro et al., 2015); Delhi, India (Kumar et al., 2018), and the researchers found that the VOC concentrations in
115 urban and suburban areas were 2-6 times higher than those at the rural area. Moreover, Li et al. (2019b) characterized the
VOCs in Zhengzhou, China and emphasized that the VOC concentrations were slightly high at the industrial site, and the
VOCs in Zhengzhou were lower than those in other Chinese cities. Therefore, simultaneous multiple-site measurements
within the city itself can provide a comprehensive understanding of VOC characteristics for policymakers to develop
effective VOC control strategies.

120 As the junction of transportation and center of industry, finance, economy and technology of East China, Shanghai covers an
area of 6340 km² and the population over 24 million. The expanding urbanization and industrialization make the VOC
pollutions in Shanghai more serious than ever before. The reported VOC pollution characteristics of Shanghai varied with
the different sampling site. For instance, the VOC concentrations varied approximately from 20 to 40 ppb at the urban area
(Geng et al., 2008; Cai et al., 2010b; Huang et al., 2015; Dai et al., 2017; Li et al., 2019c; Liu et al., 2019; Xu et al., 2019;
125 Ren et al., 2020; Wang et al., 2020; Liu et al., 2021), and ~90 ppb at the industrial area (Zhang et al., 2018; Wang et al.,
2021). However, up to now, the simultaneous observations of VOC pollution characteristics via concurrent multiple-site
measurements at Shanghai remains poorly understood, thus hindering the accurate atmospheric pollution controls. Cai et al.
(2010b) investigated the VOC pollution in Shanghai, China and highlighted that VOC concentrations in urban administrative
area (Pudong) was ~1.5 times lower than those at the industrial area (Baoshan), and slightly lower than those at the busy
130 commercial area (Xujiahui). This study provided information for understanding the characteristics of VOCs in Shanghai,
while the specific discussion about sources and secondary formation potentials of VOCs remained unclear. Moreover, the
research performed ten years ago might not reflect how land use type in the present influences in Shanghai. Therefore, it is
quite necessary to perform concurrent multiple-site and high time resolution measurements of the VOCs for their



characteristics, sources and secondary formation potentials in Shanghai.

135 Hereby, in order to distinguish the atmospheric VOCs influenced by the different land use types, we performed the concurrent online VOC measurements at three supersites. The objectives of this study are to (1) figure out the VOC characteristics influenced by the different land use types of Shanghai, (2) identify the predominate sources related to the VOCs pollution, and (3) illustrate the roles of VOCs in the formation of PM_{2.5} and O₃. The findings could advance our knowledge in the atmospheric characteristics of VOCs, as well as the relevant control methods designed for the megacity.

140 2. Measurements and methods

2.1 Sampling site description

The three sampling sites are located at the different districts of Shanghai: Jinshan district (JS site, 121.18 °N, 30.44 °E), Pudong district (PD site, 121.54 °N, 31.23 °E) and Qingpu district (QP site, 120.98 °N, 31.09 °E) (Fig. S1). The online instruments were 30 m above the ground level to avoid airflow obstruction.

145 The JS site locates in the Second Jinshan Industrial Area of Shanghai and could be regarded as an industrial site. The site locates in approximately 20 km southwest of the Shanghai Chemical Industrial Park and Garbage Disposal Incinerator-2 (Fengxian District). Moreover, a large number of chemical factories, such as rubber factories, paint solvent factories and oil refineries locate within 2 km of the JS site. In particular, Shanghai Petrochemical Industrial Limited Company (one of the largest refining-chemical integrated petrochemical companies in Shanghai) is 1.5 km southeast of the JS site. Additionally, 150 Weihong Road and Jinshan Road (the arterial road of Jinshan district) locate 100 and 300 m away from the JS site, respectively. Thus, both industrial processes and vehicle exhaust are plausible to influence the VOC emissions at the JS site.

The PD site locates in the Pudong New Area with the population up to 5.6 million (the Seventh Census of China), which is the most populous district of Shanghai, and 59 km northeast of the JS site. The BaoSteel Group Corporation, International Cruise Port wharf, Waigaoqiao Shipbuilding LTD and Domestic Waste Incinerator locate within 30 km of the PD site. The 155 Yangshan Harbor (the biggest harbor of Shanghai) and Garbage Disposal Incinerator-1 (Pudong District) locate in 51 and 37 km southeast of the PD site respectively. Furthermore, the PD site is surrounded by three main airports of Shanghai, including Hongqiao International Airport, Longhua Airport and Pudong International Airport. In addition, the site is a junction of roads, commercial and financial areas with intense human activities, which is ~1.5 km away from Jinxiu Road, Jincai High School, Jinnan High School, Jincai Experimental Primary School. Therefore, the PD site could be largely 160 influenced by the diverse anthropogenic sources, particularly the vehicle exhaust.

The QP site locates near the southeast of Dianshan Lake in the Qingpu district, and is normally taken as a city background site, which is located at 50 km northwest of the JS site and 54 km southwest of the PD site, respectively. Surrounded by vegetation and plants, the QP site situates in approximately 7.6 and 4.6 km northeast of the Grand View Garden and Chenguang Garden, respectively. Moreover, the site is 3.6 km northeast of the Qingxi Country Park and 7.5 km southwest of 165 the Zhuxi Garden. Besides, the QP site is close to Hu-Yu Highway, with a distance of approximately 1.0 km. Hence, VOC



concentrations at the QP site could be influenced by biogenic sources to some extents relative to JS and PD sites. Overall, considering the intensive traffic transportation near the sampling sites, vehicle emissions could act as an important VOC source, while the distinct surrounding environments may also lead to the varied local sources.

2.2 Sampling and analysis

170 The concentrations of VOCs, CO, NO-NO₂-NO_x, PM_{2.5}, and meteorological factors including temperature, wind speed and relative humidity (RH) were measured in one-hour resolution. The sampling campaign was performed simultaneously at the three sites from January 1 to March 31 2019.

At the JS site, the VOCs was collected and analyzed by an online gas chromatography (GC866, Chromato, France) equipped with flame ionization detector (FID). In brief, after the removal of water, the samples were separated for low-carbon (C₂-C₆) and high-carbon (C₆-C₁₂) compounds at the temperature of -5°C and 25°C, respectively. Then the gas was analyzed by FID after high temperature desorption (380°C) and column chromatographic separation. At the PD site, VOCs was measured by gas chromatography (GC580-FID, PE, USA) and TD300. The samples were separated at -30°C, after water was removed. Then the gas was determined by FID, after high temperature desorption (325°C) and column chromatographic separation. At the QP site, VOCs were determined by gas chromatography (GC5000 BTX/VOC, AMA, German) and a flame ionization detector (FID). The samples were condensed low-carbon (C₂-C₆) compounds and high-carbon (C₆-C₁₂) compounds under the temperatures of 15°C and 30°C, respectively. Then the gas was analyzed by FID after high temperature desorption (230°C) and column chromatographic separation. The R² of all of the VOCs were ≥ 0.995. The accuracy of 95 % of compounds was ≤ ± 20 %. Totally 43 species of VOCs were observed, including 16 alkanes, 11 alkenes, 16 aromatics and 1 alkyne. The minimum detection limit (MDL) of most VOC components was ≤ 0.15 ppb (Tab. S1).

185 The O₃, NO-NO₂-NO_x were characterized by trace instruments (49i ozone analyzer and 42i nitrogen oxide analyzer, produced by Thermo Environmental Instruments Inc., USA). The detection limits are 0.50 and 0.40 ppb, respectively. PM_{2.5} was monitored by a TEOM 1405-F. The meteorological variables including temperature, RH and wind speed were simultaneously acquired from a weather station about 10 km northwest of the SAES site.

2.3 Spatial analysis

190 The spatial heterogeneity of VOCs concentration at each site was determined by the coefficient of divergence (COD) (Wongphatarakul et al., 1998; Sawvel et al., 2015). The COD was calculated by the following Eq. (1):

$$COD_{jk} = \sqrt{\frac{1}{p} \sum_{i=1}^p \left(\frac{x_{ij} - x_{ik}}{x_{ij} + x_{ik}} \right)^2} \quad (1)$$

where x_{ij} presents the mass concentration in i time at the j site, j and k are two datasets, p presents the number of observations. The values of COD represented the degree of similarity of the two datasets, i.e., the value of COD approached 1, illustrating that the big difference exist in the two datasets (Song et al., 2017).



2.4 Positive matrix factorization (PMF) model

PMF was a receptor model designed for the source identification of atmospheric pollutants (Li et al., 2015b; Hopke et al., 2016; Pallavi et al., 2019). In brief, it measured the contributions and sources of pollutant by the least squares, and was based on the mass balance instead of the spectrum of source component (Yang et al., 2013; Hui et al., 2018). In the PMF 5.0, the mass balance equation was calculated by the following Eq. (2):

$$x_{ij} = \sum_{k=1}^p g_{ik} f_{kj} + e_{ij} \quad (2)$$

where x_{ij} is the j th species concentration in the sample i , g_{ik} represents the concentration of the k th source to the sample i , f_{kj} is the mass contribution of the j th species in the k th factor, e_{ij} is residue result of g_{ik} and f_{kj} , p is the number of independent sources (Paatero, 1997). The function Q was an important factor of PMF (Brown et al., 2015), and calculated by iterative minimization algorithm (Hui et al., 2018). The objective function Q was shown in the Eq. (3):

$$Q = \sum_{i=1}^n \sum_{j=1}^m \left[\frac{x_{ij} - \sum_{k=1}^p g_{ik} f_{kj}}{u_{ij}} \right]^2 \quad (3)$$

where u_{ij} is the uncertainty of j th species in the sample i .
The uncertainty of sampling was calculated by the Eq. (4).

$$Unc = \sqrt{(EF \times conc)^2 + (0.5 \times MDL)^2} \quad (conc > MDL) \quad (4)$$

where MDL is the minimum detection limit, EF is the error fraction and can be set to 0.05-0.2 (Song et al., 2007). In this study, four to eleven factors were utilized to determine the option solution. According to the results, seven factors were regarded as the greatest solution.

2.5 Potential source contribution function (PSCF) and Cluster

PSCF and Cluster were widely used to observe the back trajectories, source and direction of pollutants (Draxier and Hess, 1998; Hong et al., 2019; Liu et al., 2019), as well as designed to measure the potential VOC source and primary transport pathway of trace elements, which was derived from RTA (Ashbaugh et al., 1985; Xie et al., 2007; Zheng et al., 2018; Liu et al., 2020).

This study was determined the 24-h back trajectories (one hour interval) at the height of 500 m *via* the MeteoInfoMap software. Relevant parameters were acquired from the National Oceanic and Atmospheric Administration. The study area covered by back trajectories was divided into an array of $0.25^\circ \times 0.25^\circ$ grid cell. The higher PSCF indicated that the area was a great contributor to the VOC pollution. The PSCF could be defined as the Eq. (5).

$$PSCF_{ij} = \frac{m_{ij}}{n_{ij}} \quad (5)$$



where the m_{ij} is the number of polluted trajectories through the grid, n_{ij} is all of the trajectories through the grid. In order to distinguish the value of PSCF and increase the accuracy, the weight function W_{ij} was applied to reveal the uncertainty of small values of n_{ij} (Polissar et al., 1999). The W_{ij} could be calculated using the Eq. (6) as follows:

$$W_{ij} = \begin{cases} 1.00 & 80 < n_{ij} \\ 0.70 & 20 < n_{ij} \leq 80 \\ 0.42 & 10 < n_{ij} \leq 20 \\ 0.05 & n_{ij} \leq 10 \end{cases} \quad (6)$$

2.6 Secondary organic aerosol formation potential (SOAFP)

As discussed by Grosjean and Seinfeld (1989), SOAFP could be used to evaluate quantitatively the VOC influences on the secondary aerosol formation based on a variety of assumed interactions between VOCs and OH under the sun-light irradiation (8:00-17:00).

$$SOAFP_i = [VOC_i] \times FAC_i \quad (7)$$

where VOC_i is the concentration of the i VOC species, FAC_i is fraction aerosol coefficient of the i compound. The FAC_i was obtained from the previous studies (Grosjean and Seinfeld, 1989; Zhu et al., 2017; Mozaffar et al., 2020).

2.7 Ozone formation potential (OFP)

The photochemical activity of VOCs was normally assessed by the O_3 formation potential (OFP) (Niu et al., 2016). The value of OFP was effected by many factors like meteorological conditions, VOC concentrations and VOC sources. The OFP was calculated by the following Eq. (8):

$$OFP_i = [conc]_i \times MIR_i \quad (8)$$

where OFP_i is the ozone formation potential of the i species, $[conc]_i$ is the concentration of VOC species i , MIR_i is the maximum incremental reactions of the i VOC species, as reported by Carter (1994).

2.8 Sensitivity analysis

In order to further understand the relationship between VOCs and O_3 , a gradient model was applied to investigate the sensitivity of O_3 pollution to the VOC concentration. The Eq. (9) was below:

$$\eta = \frac{\Delta_{VOCs}}{\Delta_{O_3}} \quad (9)$$

where Δ_{VOCs} and Δ_{O_3} is the concentrations of VOCs and O_3 in the specific O_3 gradients, respectively. The characteristic



structure and reactivity could influence the contribution of VOCs to O₃ formation (Cater, 1994). To determine the quantitative relationship between the VOCs and O₃, the VOCs-sensitivity coefficient (VOCs-S_{O₃}) was used as the Eq. (10):

$$VOCs-S_{O_3} = \frac{\Delta_{VOCs} / B_{VOCs}}{\Delta_{O_3} / B_{O_3}} \quad (10)$$

250 where B_{VOCs} and B_{O_3} are the background concentrations of VOCs and O₃. The O₃ concentrations below 100 μg m⁻³ were averaged to be the background level. The background concentration of VOCs (B_{VOCs}) was the corresponding VOC concentrations. The high value of VOCs-S_{O₃} implied that the concentration of VOCs was greatly affected by the variations of O₃ concentration. In order to quantify the sensitivity of VOCs to O₃, VOCs and O₃ were classified into different groups with a O₃ concentration interval of 5 μg m⁻³. It could be calculated by the Eqs. (11-14):

$$y = a \cdot x^b \quad (11)$$

255 $\ln y = b \cdot \ln(a \cdot x) \quad (12)$

$$\ln VOCs - S_{O_3} = b \cdot \ln a + b \cdot \ln \frac{\Delta_{O_3}}{B_{O_3}} \quad (13)$$

$$\ln \frac{\Delta_{VOCs}}{B_{VOCs}} = k \cdot \ln \frac{\Delta_{O_3}}{B_{O_3}} + c \quad (14)$$

260 where k represents the linear coefficient between $\ln(\Delta_{VOCs}/B_{VOCs})$ and $\ln(\Delta_{O_3}/B_{O_3})$, c is the intercept. The method was also applicable to the calculation of VOCs-S_{PM_{2.5}}, the background concentration of PM_{2.5} ($B_{PM2.5}$) was determined by that less than 20 μg m⁻³ (Han et al., 2017). More details can be found in Han et al. (2017). This method was appropriate for understanding the sensitivity of VOC pollution level to O₃ (or PM_{2.5}) at polluted environments.

3. Results and discussion

3.1 Characteristics of air pollutants

3.1.1 Data overview

265 The time series of meteorological factors, VOC categories, PM_{2.5} and O₃ are shown in Fig. 1. During the observation campaign, 60 VOC species including 32 alkanes, 11 alkenes, 16 aromatics and 1 alkyne were measured. The temperatures were averaged to be 8.69 ± 3.24, 9.02 ± 3.24 and 7.73 ± 2.92°C, and the hourly mean RH were 83.77 ± 11.38, 75.37 ± 13.29 and 71.80 ± 9.28 % at the JS, PD and QP sites, respectively. The wind speed ranged from 0.86 to 3.39, 0.60 to 4.78 and 2.03 to 8.89 m sec⁻¹ with the averages of 1.91 ± 0.49, 1.30 ± 0.62 and 4.37 ± 1.47 m sec⁻¹ at the JS, PD and QP sites, respectively.

270 Under the similar temperature and humidity conditions, the QP site presented higher wind speed than those of the JS and PD sites, and the large gap could be used to explain the distinct VOC characteristics, as discussed later. The results of wind speed were higher than those obtained in Shanghai, China (Zhang et al., 2018), Zhengzhou, China (Li et al., 2019b) and



Xi'an, China (Song et al., 2021).

The VOC concentrations ranged from 7.65 to 71.07, 7.87 to 47.52 and 3.79 to 33.36 ppb with the averages of 21.39 ± 12.58 , 21.36 ± 8.58 and 11.93 ± 6.33 ppb at the JS, PD and QP sites, respectively. Obviously, the mean VOC concentrations at the QP site were approximately twice lower than those of the JS and PD sites, due to the emission strength and atmospheric diffusion condition. The VOC levels measured were comparable with those measured in London, England (22.1 ppb), while lower than those observed in Houston, USA (33.88 ppb), Los Angeles, USA (41.3 ppb) and Tokyo, Japan (43.3 ppb) (Hoshi et al., 2008; Schneidmesser et al., 2010; Warneke et al., 2012; Sadeghi et al., 2021). Also, the VOC concentrations shown herein was comparable or lower than those of other studies relevant to China. For instance, the studies in Wuhan (22.2 ppb) (Hui et al., 2018), Chongqing (24.0 ppb) (Li et al., 2018) and Hong Kong (12.7 ppb) (Liu et al., 2019) showed that the VOC concentrations were similar with ones in the present study. However, the present result was lower than those reported by the studies in Nanjing (29.6 ppb) (Shao et al., 2016), Zhengzhou (28.8 ppb) (Li et al., 2019b), Heshan (29.3 ppb) (Song et al., 2019a) and Xi'an (33.8 ppb) (Song et al., 2021). Additionally, compared with the relevant measurements performed previously in Shanghai at the same sampling sites, this study presented lower VOC concentrations. In detail, at the JS site, the VOC concentration was approximately 4 times lower than the findings of Zhang et al., (2018) (94.14 ppb). At the PD and QP sites, the results in this study were slightly lower than those obtained by Cai et al. (2010b) (24.3 ppb) and Zhang et al. (2020a) (15.41 ppb). Changes in meteorological conditions and boundary layer height were the important reasons for this phenomenon. For instance, the occurrence of high wind speed, which was usually accompanied with better convection conditions, resulted in the relatively decreasing VOC levels. Furthermore, a variety of control strategies, such as prohibition of fireworks in the open air and strengthening VOC detection standards and control technology, especially in the Shanghai Baosteel Group Corporation, Shanghai Chemical Industrial Park and Shanghai Petrochemical Industrial Limited Company, and the system of "one factory, one strategy", targeted at mitigating VOC emissions were implemented by Shanghai government.

The maximum VOC concentrations appeared on the 23 January at the JS and PD sites and 27 January at the QP site, respectively. According to the Shanghai Municipal Bureau of Statistics (<http://tjj.sh.gov.cn>), the traffic flow in January was ~10 % higher than that in the following two months. The phenomenon was likely attributed to the Spring Festival Travel rush, i.e., population travel intensively occurred around the Chinese Spring Festival, thereby causing the elevated pollutant emissions. However, the minimum values presented in the 5, 10 February and 18 March at the JS, PD and QP sites, respectively. The result was due to the fact that a large number of organizations surrounding the sampling sites, such as schools, factories, shopping malls and institutes, were closed for celebrating Chinese Spring Festival, thus causing the decreased concentrations of VOCs especially in aromatics (mainly benzene and toluene) at the JS and PD sites in the February. The reduced VOC concentrations coincide to the response of varied atmospheric pollutants to the COVID-19 lockdown that occurs one year later (Pakkattil et al., 2021), suggesting that the human activities might indeed greatly affect the atmospheric pollution characteristics. Compared with the JS and PD sites, the minimum VOC value at the QP site obviously appeared at different time, suggesting that the impact of local source strength on VOC pollution was varied. It is



worth noting that the distinct spatial heterogeneity of VOCs was observed with the highest value of the coefficient of divergence ($COD = 0.36$), appeared between the JS and QP sites, followed by the PD and QP sites ($COD = 0.33$), with that between the JS and PD sites ($COD = 0.20$) being the lowest. Hence, the spatial heterogeneity of VOCs between the JS and PD site was narrow, while the QP site is largely different from other two sites at the pollution level. This phenomenon was because there were similar VOC emission intensity and atmospheric stability at the JS and PD sites, both of which showed obvious discrepancies at the QP site.

During the observation period, the average $PM_{2.5}$ values were 45.57 ± 27.59 , 48.51 ± 27.22 and $40.27 \pm 27.78 \mu\text{g m}^{-3}$, and the mean O_3 concentrations were averaged to be 73.59 ± 23.59 , 57.48 ± 20.49 and 99.30 ± 24.00 ppb at the JS, PD and QP sites, respectively. The minimum hourly $PM_{2.5}$ levels were observed in 31 March at the JS site, 6 and 10 February at the PD and QP sites with the values of 10.67, 12.33 and $7.44 \mu\text{g m}^{-3}$, respectively, while the relatively high O_3 concentrations and low VOC concentrations were determined. Statistically, VOCs were found to be positively correlated with $PM_{2.5}$, due to the fact that VOCs were a significant precursor of $PM_{2.5}$. It was well documented that the elevated VOC concentrations led to the increasing rate of $PM_{2.5}$ production *via* photochemical oxidation, gas-particle partition and heterogeneous absorption (Seinfeld et al., 2001; Yang et al., 2015; Han et al., 2017). Moreover, there was homology between the VOCs and $PM_{2.5}$ to a certain degree. For instance, Wu et al. (2019) showed that the predominant source of $PM_{2.5}$ was the traffic exhaust in South Korea. Meanwhile, a multitude of studies showed the traffic-related source was the dominating source of VOCs including Shanghai, China (Liu et al., 2019), Chongqing, China (Li et al., 2018), Beijing, China (Li et al., 2016), Paris, France (Gaimoz et al., 2011) and Hawthorne, USA (Brown et al., 2007). However, the VOC concentrations were negatively correlated with O_3 . The termination and titration ($NO + O_3 \rightarrow NO_2 + O_2$) were more efficient and lots of factors, rather than the emission of precursors, impacted on the surface O_3 . Li et al. (2019b) emphasized that the absolute concentration of precursor was not the only factor during the O_3 formation in Zhengzhou, China. Additionally, the ratio of VOCs/ NO_x was less than 5.5 at three sampling sites, suggesting that there was a VOC control system i.e., O_3 formation was sensitive to VOCs and a higher proportion of OH radical reacted with NO_2 to suppress the O_3 formation. Therefore, the reduction of VOCs might be partly attributed by the chemical loss pathway, and counteraction was imposed by uncertain factors during the formation of O_3 .

3.1.2 Chemical compositions

The VOC compositions at the JS, PD and QP sites are presented in Fig. 2. During the sampling period, the most abundant species were alkanes, followed by aromatics, and the contributions of alkenes and alkyne were close at the above sites. Specially, ethane, propane, iso-butane, n-butane, ethylene, benzene, toluene and ethyne were the most abundant compositions, contributing to $> 75\%$ of TVOCs (total VOCs), suggesting the strong vehicle-related source at three sampling sites.

Among the four major organic classes, the fractions of alkanes were 49, 71 and 61 % at the JS, PD and QP sites, respectively. Analogously, Zhang et al. (2020a) investigated the contribution of VOC categories to the TVOCs in Shanghai, China, and



340 showed that the largest contribution was alkanes, comprising 59.36 % of the total VOCs, due to their widespread emission
sources and longer atmospheric lifetime. The great contributions of ethane, propane and C₄-C₆ branches alkanes led to the
highest proportions of alkanes at the three sites, as the findings of Zhang et al. (2020a) and Song et al. (2021), while the
relative abundances of the compounds varied with the sampling sites. The fraction of alkanes at the PD site was obviously
345 higher than those at the JS and QP sites, which was mainly contributed by the obvious high proportion of propane at the PD
site. This phenomenon was greatly influenced by the vehicle emission, and the PD site was situated at the junction of roads,
metros, commercial and financial areas, which was ~1.5 km away from Jinxiu Road and metro line 6 and ~2 km away from
the Waihuan Highway. Moreover, the contribution of ethane at the JS site was nearly half lower than that at the PD and QP
sites. Ethane is a major compound of natural gas, which is associated with the incomplete combustion (Guo et al., 2011). It
was thus supposed that the vehicle emission exerted a relatively weak influence on VOC emission at the JS site, as compared
350 to the other two sites.

The second-largest group was aromatics accounting for 21, 11 and 14 % at the JS, PD and QP sites, respectively. As reported
by Cai et al. (2010a), aromatics was found to be abundant species in addition to alkanes, accounting for 24.9 % of the total
VOCs at the Xujiahui site in Shanghai, China, which was slightly higher than the results obtained in this study. Note that the
dominating compounds of aromatics were toluene, m/p-xylene, benzene, ethylbenzene and o-xylene (BTEX), and the result
355 was in line with that in Shanghai, China (Zhang et al., 2018) and Xi'an, China (Song et al., 2021). The proportion of
aromatics at the JS site was approximately twice greater than those at the PD and QP sites. In particular, the contribution of
toluene at the JS site was markedly increased (~3 times) relative to the other two sites. Similarly, Li et al. (2019b) studied the
VOC concentrations at different sites in Zhengzhou, China, and showed that the fraction of toluene was approximately twice
higher at the JK site (an industrial site) than those at the other sites. The JS and JK sites are close to the industrial area and
360 have heavy industrial emissions. The industrial activities in paint and printing factory, manufacturing factory and rubber
factory were the potential reason for such phenomenon (Zheng et al., 2010; An et al., 2014; Debevec et al., 2021).

The alkenes accounted for 15, 10 and 11 % at the JS, PD and QP sites, respectively, and the discrepancies of alkenes
contribution to TVOCs among three sites were narrow. The ethene, propylene and butene were predominant compounds in
the specie of alkenes, and their contributions were comparable to the results of Shao et al. (2016). Meanwhile, the alkyne
365 contributed 15, 8 and 14 % on the TVOCs at the above sites. Compared with the result reported by Liu et al. (2017) in
Hangzhou, China, the contribution of alkyne was comparable to the present study, accounting for 16.6 % of the TVOCs. As
shown in Fig. 2, the fraction of alkyne was twice lower at the PD site than that at the JS and QP sites, which may be caused
by the weak combustion sources including chemical- and bio-fuels burning (Zhu et al., 2016; Li et al., 2019b).

3.1.3 Diurnal variations

370 The diurnal variations of VOCs on the weekdays and weekends at the JS, PD and QP sites are shown in Fig. 3. On the
weekdays, the average VOC concentrations were 21.03 ± 2.66 , 22.00 ± 4.88 and 11.09 ± 1.58 ppb at the JS, PD and QP sites,
respectively, whereby the highest peaks were observed during the rush-hour traffic in the morning (8:00-10:00 LT), reaching



26.61, 35.11 and 13.54 ppb. The highest peak was more significant at the PD site than those at the JS and QP sites, illustrating that the vehicular emission accounted for more VOC emissions at the PD site than those at the other two sites.

375 During the rush-hour traffic in the evening (18:00-21:00 LT), the VOC concentrations also intended to increase, and the values were 18.46, 20.82 and 10.22 ppb at the JS, PD and QP sites, respectively. Such results could be attributed to the strong influence of the vehicle exhaust. The VOC concentrations dropped to the minimum at the 16:00 LT with the values of 16.96, 15.62 and 8.77 ppb at the JS, PD and QP sites, respectively. The strong radiation, high temperature and boundary layer resulted in the most intense air convection condition and promoted the photochemical loss and dilution of VOCs,

380 leading to the lowest VOC concentration (Zhang et al., 2018). It is worthwhile to note that the VOC concentrations remained relatively high value in the early morning (around 5:00 LT) at the JS site compared with those at the other two sites. This phenomenon was attributed to the fact that a large number of rubber factories, paint solvent factories and oil factories located within 2 km of the JS site, whereby some factories usually work continuously for 24 hours, leading to the increased VOC concentrations. Compared with the previous studies (Velasco et al., 2007; Zhang et al., 2018; Wang et al., 2021), the diurnal variation of the VOC concentrations in this study did not show apparent bimodal feature at the sampling sites. The industrial processes and biogenic emission surrounding the sampling sites also had great influence on the VOC variations except for the traffic exhaust, which was the potential reason for such scenario. Therefore, it is necessary to analyze the diurnal variation of VOC concentrations at the different land-use types.

385

On the weekends, the JS site exhibited the highest average VOC concentration of 20.36 ± 2.23 ppb, followed by the PD and QP sites with the concentrations of 19.96 ± 2.37 and 10.96 ± 0.67 ppb, respectively. The VOC concentrations on the weekends were 3.31, 10.19 and 1.19 % lower than those on the weekdays. Similarly, the elevated VOC concentrations on the weekdays were found in other cities including Shanghai, China (Geng et al., 2008), Sacramento (Murphy et al., 2007) and Los Angeles, USA (Nussbaumer and Cohen, 2020), due to the low anthropogenic activities occurring on the weekends, reflecting the low VOC emission (Murphy et al., 2007). It should be noted that there were narrow discrepancies of VOC concentrations at the JS site between the weekdays and weekends except for the rush hour in the morning, which was attributed to the influence of the continuous operation of industrial processes. At the PD site, the highest value during the morning peak on the weekends (26.03 ppb) was obviously lower than that on the weekdays (~34.88 % decreased). Such scenario resulted from the enhancement of anthropogenic VOC emissions intensity on the weekdays, suggesting that there were anthropogenic-dependent VOC emissions at the PD site. At the QP site, the elevated VOC concentrations were presented during the 18:00-20:00 CST on the weekends relative to the weekdays. The phenomenon was associated with the fact that a large number of people had a trip around the QP site on the weekends, leading to the VOC emissions increased. Furthermore, the VOC concentration gradually increased during the rush-hour traffic in the morning and evening both on weekends and weekdays. Additionally, the minimum VOC concentrations occurred around the same time, which appeared on the 16:00 CST at the JS and PD sites and 15:00 CST at the QP site on the weekends, respectively, with the values of 17.14, 17.56 and 10.33 ppb. Such phenomenon could be explained by the meteorological factors, and would be expounded in detail in the last section.

390

395

400

405



3.1.4 Clean-haze discrepancy

Referring to the previous documents (Li et al., 2017; Hui et al., 2019), haze pollution was defined as the condition with visibility < 10 km and RH > 80 %. During the observation period, there were three sequential haze pollution events at the three sites on the basis of this criteria, i.e., 18 to 25 January, 23 February to 3 March and 21 to 26 March. Note that the haze break was usually accompanied with the increasing VOC concentrations. The VOC concentrations between the clean and polluted days are shown in Fig. 4. The VOC concentrations on the clean days were averaged to be 20.53 ± 12.10 , 19.29 ± 7.60 and 11.04 ± 6.67 ppb at the JS, PD and QP sites, respectively. When it comes to haze days, the VOC concentrations increased by 27.15, 32.85 and 22.42 % at the JS, PD and QP sites, respectively. Wu et al. (2016) also emphasized the increased VOC concentrations during the haze days relative to clean days in Beijing, China. Obviously, the ‘haze-clean’ discrepancy of VOC concentrations was narrow at the QP site compared with the JS and PD sites. Such phenomenon could be attributed to the rapid industrialization and urbanization, resulting in the stagnant weather conditions and high anthropogenic emissions, which further led to the severe haze pollution at the JS and PD sites. In detail, the ‘clean-haze’ discrepancy was dominated by the aromatics (*m*-ethyltoluene, *p*-ethyltoluene, *m*-ethylbenzene, 1, 2, 4-trimethylbenzene) at the JS and PD sites, as reflected by the 44.54 % and 36.05 % higher concentrations on haze days relative to clean days. The elevated concentrations reflected the concentrated emission sources of industrial production, painting/coating and vehicle exhaust. Zhang et al. (2021) studied the VOC characteristics during the haze pollution in Zhengzhou, China, and showed that aromatics present an upward tendency (~34.04 % uplift) on the haze days, which was slightly lower than the results shown herein. at the QP site, alkanes (2, 2, 4-trimethylpentane, *n*-hexane, *n*-heptane) presented significant ‘clean-haze’ discrepancy (~36.58 % uplift), implying the great influences of vehicle exhaust and fuel evaporation. By contrast, Hui et al. (2018) observed the elevated concentration of alkanes during the haze days in Wuhan, China, and found that there were 37.28 % increment of alkanes, which was comparable to the result in the present study. Thus, it could be deduced that, the haze occurrence is mainly associated with vehicle exhaust, industrial production and painting/coating at the JS and PD sites, whereas the vehicle exhaust and fuel evaporation at the QP site. The result agreed well with the studies about the haze pollution in Shanghai, China (Li et al., 2019b; Wei et al., 2019). Accordingly, VOC species could probably serve as the source indicators when exploring the haze pollution.

3.2 Source apportionment

3.2.1 Special VOC ratio analysis

Different VOC species have different sources, and accordingly the ratio of different species could be used to preliminary distinguish the emission sources (An et al., 2014). Herein, the characteristics of toluene/benzene (T/B), *iso*-pentane/*n*-pentane (P/P) and *m*, *p*-xylene/ethylbenzene (X/E) varying the sampling sites to identify the source types. The results are shown in Fig. 5 and Fig. S2-4.

It was well documented that the varied VOC sources could be identified by the different T/B ratios. The ratio in the range of



0.2-0.4 indicates different combustion processes (Li et al., 2011; Mo et al., 2016). The ratio in the range of 0.9-2.2 indicates
440 the vehicle sources varying with fuel types (Dai et al., 2013; Zhang et al., 2013; Yao et al., 2015; Deng et al., 2018). The T/B
ratio about vehicle emission exhibited approximately 1.5, which approaches the results of the tunnel experiments, due to the
different vehicle emissions including diesel and gasoline vehicle emissions (Deng et al., 2018; Song et al., 2021). The ratio in
the scope of 1.4-5.8 reflects the industrialization impact (Mo et al., 2015; Shi et al., 2015). In addition, the ratio greater than
8.8 implies the effect of paint solvent usage (Yuan et al., 2010; Zheng et al., 2013). The mean T/B ratios were 4.59 ± 4.3 ($r =$
445 0.41) and 1.61 ± 0.79 ($r = 0.65$), respectively at the JS and PD sites, with most of the ratios (68.89 and 84.15 %) distributing
the reference range of vehicle emissions and industrial emissions, suggesting that both sources exerted a significant influence
on VOC concentrations (Fig. 5a-b). It is worth noting that the range of T/B ratios at the JS site (0.44-22.86) were wider than
that at the PD site (0.48-4.38), suggesting that the VOC concentrations at the JS site were influenced by diverse emission
factors. The average ratio at the QP site was 1.01 ± 0.66 ($r = 0.70$) with 43.02 % of T/B ratios distributing the range of
450 vehicle emissions and burning emissions, suggesting that both of the sources contributed significantly to VOC pollution (Fig.
5c). The temporal variations of T/B ratio and TVOC concentrations are shown in Fig. S2. The T/B ratios were mainly located
in the scope of 0.9-2.2 and 1.4-5.8 at the JS and PD sites during the high VOC concentrations, respectively; while the
specific values at the QP site were only concentrated in the scope of 0.9-2.2. Such phenomenon showed that vehicle exhaust
was a significant contributor to the VOC pollution at the three sampling sites, and VOC concentrations were less influenced
455 by the industrial emission at the QP site relative to the JS and PD sites, due to the fact that the QP site was normally taken as
a city background site and far from the industrial park.

The fossil-fuel-derived sources (vehicle exhaust, fuel evaporation and coal combustion) could be further distinguished by the
P/P ratio. Iso-pentane and n-pentane have similar atmospheric lifetimes, and therefore are significantly correlated, as
evidenced by the linear relation coefficients (r) were 0.91, 0.91 and 0.82 ($p < 0.01$) at the JS, PD and QP sites, respectively.
460 The phenomenon supported the fact that the two compounds varied with a similar trend and had constant emission sources
(Jobson et al., 1998; Yan et al., 2017). Lower P/P ratios (0.56-0.80) are often identified for coal combustion (Li et al., 2019a),
and it was well known that the P/P ratios in the range of 2.2-3.8 are characterized by vehicle emission (Liu et al., 2008; Wang
et al., 2013). Figure 5d shows that the linear correlation coefficients between the iso-pentane and n-pentane were 0.96 ± 0.30
($r = 0.91$), 1.36 ± 0.22 ($r = 0.91$) and 2.46 ± 1.49 ($r = 0.81$) at the JS, PD and QP sites, respectively. The result at the QP site
465 was comparable to that measured at a Pearl River tunnel (2.93), suggesting that the vehicle emission is an outstanding VOC
source (Liu et al., 2008). The lower ratios at the JS and PD sites highlighted the mixed emission sources with significant coal
combustion included. The temporal variations of P/P ratio and TVOC concentrations are shown in Fig. S3. The P/P ratios
were approaching 2.2-3.8 at the sampling sites during high VOC values, indicating the great impact of vehicle emission on
VOC pollution, in accordance with the findings of Song et al. (2021).

470 Besides the local emissions influencing the VOC pollution characteristics, regional transport has been probed as a potential
VOC source. Herein, the ratio of X/E was used to evaluate the transport impacts. *M*, *p*-xylene and ethylbenzene are found to
be similar in emission sources, while the former exhibits ~3 times greater reactivity toward OH radical than the latter



(Nelson and Quigley, 1983; Chang et al., 2006; Vardoulakis et al., 2011). Hence, lower X/E ratios normally suggested more significant air mass aging, that is, more influences from external transport. The X/E ratios were averaged to be 2.33 ± 0.37 ($r = 0.98$), 2.18 ± 0.42 ($r = 0.97$) and 2.03 ± 1.52 ($r = 0.74$) at the JS, PD and QP sites, respectively (Fig. 5e). The results showed that the X/E ratios were similar at the sampling sites while the values were slightly lower at the QP site relative to the JS and PD sites, indicating that the aged VOCs contributed by the polluted air masses *via* the regional transport toward the QP site. The temporal variations of the X/E ratio and TVOC concentrations are shown in Fig. S4. During the VOC pollution, the X/E ratios were approximately 2.3, 2.5 and 1.8 at the JS, PD and QP sites, respectively. Obviously, the X/E ratio was lower at the QP site than those at the JS and PD sites. In particular, the high VOC concentration (27.17 ppb) was observed in 7 February at the QP site, corresponding to the minimum X/E ratio (0.27), while the X/E ratios were 3.07 and 1.95 at the JS and PD sites, corresponding to the VOC concentrations of 12.45 and 22.45 ppb. Such results illustrated that the influence of external transport during the high VOC concentrations was greater at the QP site compared with the JS and PD sites.

3.2.2 The PMF analysis

The PMF analysis can quantitatively determine the VOC source contributions, compared with the specific VOC ratio analysis (Hui et al., 2019). In this study, 39 VOC species were put into the PMF model, followed by the output of seven resolved factors including vehicle exhaust, industrial source, LPG usage, paint solvent, fuel evaporation, coal combustion and biogenic source. The factor profiles and contributions to VOCs at the JS, PD and QP sites are shown in Fig. 6.

Vehicle exhaust was characterized by the high proportions of alkanes, some alkenes and certain percentage of aromatics (benzene, xylene and trimethylbenzene) (Liu et al., 2008; Cai et al., 2010; Ling et al., 2011; An et al., 2017; Hui et al., 2018). In this study, the high contributions of the ethane (69.59 and 48.01 %), *iso*-butane (35.14 and 26.12 %) and some alkenes especially the propylene (34.72 and 19.74 %) and *trans*-2-butene (50.49 and 17.40 %) at the JS and PD sites, as well as the ethane (42.41 %), ethylene (49.14 %) and ethyne (45.94 %) at the QP site were observed, and all of these compounds are widely regarded as vehicular emission tracers (Cai et al., 2010a; Ling et al., 2011; An et al., 2017; Hui et al., 2018). The vehicle contributions were 23.18, 33.37 and 32.12 % at the JS, PD and QP sites, respectively, indicating that vehicle exhaust was the predominant source of VOCs, as the results of T/B and P/P ratios mentioned above. Shanghai owns the motor vehicles more than 4.4 million at 2019, and vehicle exhausts had been proved to be one of the main causes of the local air pollution in Shanghai (Huang et al., 2015; Dai et al., 2017; Liu et al., 2019; Cai et al., 2010b).

Industrial emission was featured by high percentage of aromatics (benzene, toluene and trimethylbenzene) and certain percentage of alkanes and alkenes (Guo et al., 2011; Dumanoglu et al., 2014; Sun et al., 2016). At the JS and PD sites, the high contributions of *n*-nonane (17.84 and 33.99 %), benzene (13.89 and 39.16 %), toluene (21.11 and 19.54 %), trimethylbenzene (94.18 and 84.05 %), hexane (14.81 and 38.96 %) and ethylene (14.99 and 36.91 %) were observed. It was widely acknowledged that asphalt could release *n*-nonane, which was mainly used in industrialization and transportation (Brown et al., 2007; Liu et al., 2008). Moreover, benzene and toluene are primarily applied for industrial solvent production,



and trimethylbenzene is frequently used in manufacturing (Morrow, 1990; Ling et al., 2011). Therefore, the recognized factor can be identified as industrial source. Industrial events were calculated to contribute 22.39 % of the VOCs at the JS site, as well as 18.81 % at the PD site, indicating the considerable contributions of industrialization next to the aforementioned traffic factors. The QP site is far away from the industrial area, and therefore no industrial factors were disclosed at this site.

510 Coal combustion factor was characterized by propane, ethylene, ethyne, and benzene (Liu et al., 2008; Ling et al., 2011; Song et al., 2018). Moreover, the relatively low proportions of propene, *n*-hexane, *n*-heptane and toluene should be considered as well due to their detectable levels in the coal combustion processes (Hui et al., 2018). The PMF analysis illustrated that coal combustion was the third-largest source of VOCs at the three sites, due, in part, to a variety of combustion methods. Coal combustion is responsible for 14.95 % of the VOC emission at the PD site, as well as 13.85 % at the QP site. However, the proportion reached up to 21.48 % at the JS site, reflecting the frequent fossil usage in the industrial area of Shanghai.

LPG usage was determined by some alkanes (propane, *n*-butane and *iso*-butane) and alkenes (ethylene, propylene and butene). At the JS and PD sites, high proportions of propane (21.24 and 14.41 %), *n*-butane (15.53 and 13.79 %), *iso*-butane (12.61 and 11.40 %), ethylene (31.18 and 10.08 %) and propylene (34.94 and 31.38 %) were observed, as well as the *iso*-butane (43.88 %), propylene (25.08 %) and *cis/trans*-2-butene (53.10% and 57.65 %) at the QP site, highlighting the LPG-related sources (Yang et al., 2013; Lyu et al., 2016). Herein, LPG usage explains 13.17, 14.76 and 12.14 % of the VOCs monitored at the JS, PD and QP sites, respectively. At the end of 2015, the amount of LPG users about household and catering achieved 3.3-6.5 million in Shanghai (Hui et al., 2018; Zhang et al., 2018a). Overall, LPG usage was one of the important VOC sources, and its VOC contributions accounted for the half of the vehicle emissions.

525 Fuel evaporation can be identified by C₃-C₇ alkanes, especially *n*-pentane and *iso*-pentane (Zheng et al., 2020), as well as the C₃-C₅ alkenes such as *trans/cis*-2-butene (Geng et al., 2009; Hui et al., 2018; Zhang et al., 2018a; Zheng et al., 2020). There were high percentages of *n*-pentane (37.94, 25.20 and 71.95 %), *iso*-pentane (41.45, 28.18 and 23.16 %) and butene (26.73, 70.83 and 22.52 %) at the JS, PD and QP sites, respectively. Some literature showed that alkanes like *n*-pentane and *iso*-pentane were gasoline tracers, and some low-carbon alkanes could evaporate from the unburned fuels (Guo et al., 2004; Wang et al., 2013). The VOC contributions from fuel evaporation were calculated to be 4.62, 10.35 and 20.15 % at the JS, PD and QP sites, respectively.

535 Paint solvent usage is normally characterized by C₆-C₈ alkanes and some aromatics like toluene, ethylbenzene and *o/m/p*-xylene (An et al., 2017; Hui et al., 2018; Song et al., 2019a). Wang et al. (2013) further proposed that these aromatic compositions could be emitted from the usages of painting, adhesives, and coating activities. Herein, emission factors that meet the characteristics could be explained by paint solvent usage, which accounted for 15.15, 7.77 and 10.36 %, respectively at the JS, PD and QP sites.

Biogenic source was distinguished by a high contribution of isoprene (Liu et al., 2008; Wu et al., 2016). Factors that coincide to the specific characteristic were regarded as biogenic source in this study. Our analysis indicated that biogenic source could explain 11.39 % of the VOCs at the QP site, reflecting the vegetation surrounding this site. However, this emission factor



540 could not be reproduced when it comes to the analysis of the JS and PD sites, implying the limited influences of biogenic
sources in the population- and industrialization-concentrated areas that were suffered from the anthropogenic emissions.
Generally, the contribution from vehicle exhaust at the sampling sites accounted for nearly one third of total VOC sources.
Obviously, the vehicle contribution at the JS site was lower than those at the PD and QP sites, which could be attributed to
the heavier emissions of industrial production and coal combustion at the JS site. Moreover, vehicular emission was also a
545 dominating source of VOCs in other cities, and the contributions were higher than 20 % except in Calgary, Canada (17.2 %)
(Fig. 7). The effective and continuous control strategies about vehicle exhaust were still of priority to alleviate VOC
pollution in Shanghai. The fraction of industrial source was the second-largest source at the JS and PD sites, which were
relatively high compared with the other studies, except for Xi'an, China (29.7 %) and Paris, France (35 %). This was
partially due to the fact that the JS site located in Second Jinshan Industrial Area of Shanghai and could be regarded as an
550 industrial site, and Waigaoqiao Ship building LTD and BaoSteel Group Corporation located within 30 km of the PD site,
illustrating the great influence of industrial processes on VOC pollution at the JS and PD site. Combustion was the
third-largest source at the three sites, and its contribution varied largely in different studies, from 4 % (Song et al., 2019b) to
46 % (Bari and Kindzierski, 2018), which was ascribed to the different definition of the combustion among various studies.
For instance, Song et al. (2019b) only regarded the wood combustion as the combustion source in the study of Seoul, South
555 Korea, while the sum of fuel combustion and oil/natural gas extraction/combustion were referred to the combustion source in
the study of Calgary, Canada (Bari and Kindzierski, 2018).

The contribution of fuel evaporation varied by site locations, i.e., at the JS site (4.62 %) was lower than that in the previous
studies (6.28-20 %), while the value at the PD site (10.35 %) was relatively average (Li et al., 2018; Hui et al., 2018; Liu et
al., 2019; Song et al., 2019a, b; Song et al., 2021). At the QP site, the result (20.15 %) was comparable with that in the other
560 studies (Hui et al., 2018; Li et al., 2018; Song et al., 2019a, b; Song et al., 2021). The proportions of LPG usage were
approximately twice higher at the sampling sites than those reported by the other studies (Hui et al., 2018; Song et al.,
2019a). The fractions of paint solvent usage shown herein were lower than the average of other cities (8.2-41 %) (Gaimoz et
al., 2011; Bari and Kindzierski, 2018; Li et al., 2018; Liu et al., 2019; Hui et al., 2018; Song et al., 2019a, b; Liu et al., 2021;
Song et al., 2021). The contribution of biogenic source at the QP site was relatively average, compared to the estimates from
565 other studies (4.9-15 %) (Cai et al., 2010b; Gaimoz et al., 2011; Bari and Kindzierski, 2018; Hui et al., 2018; Li et al., 2018;
Song et al., 2019a, b). Obviously, the results of source contribution estimates varied with different studies (Lyu et al., 2016;
Li et al., 2020). Additionally, the VOC sources also showed different at a regional scale within the city (Tang et al., 2008; Li
et al., 2019b; Cai et al., 2010; Song et al., 2021). Such phenomenon was partially due to the different factors during the
observation period, inclusion of VOC species, emission strength and/or land-use types (Li et al., 2019b; Cai et al., 2010; Li
570 et al., 2020; Song et al., 2021). Thus, the source apportionment for the different land-used types at a regional scale among
various studies is necessary to identify the high-quality localized source.

3.3 Back trajectories and PSCF results



575 Regional transport could also contribute to VOC pollution, besides the direct influence of local source (Hui et al., 2018).
Figure 8 exhibited the 24-h backward trajectories, PSCF results and the VOC proportion of each trajectory during the entire
observation at the JS, PD and QP sites. There were 6 clusters (northern trajectories: Cluster 1 + 2; eastern trajectories:
Cluster 3; southern trajectories: Cluster 4; southwestern trajectories: Cluster 5; northwestern trajectories: Cluster 6) at the JS
site, as shown in Fig. 8a. One can see that the contributions of northern trajectories to both the total trajectories and the total
pollution trajectories were significantly higher than other four cluster trajectories, comprising 45.74 and 46.46 %,
580 respectively (Tab. 1). Identified as the north direction cluster, the north long-distance trajectory (Cluster 1) and short-distance
trajectory (Cluster 2), respectively, accounting for 16.67 and 29.07 % of the VOC transportation, indicating that the VOC
pollution was mainly impacted by the northern trajectories from the junction of the Bohai Sea, Shandong Province, the East
China Sea and Jiangsu Province in addition to local emissions. The contributions of VOCs by each air mass trajectories
indicated that alkanes tended to dominate the transported VOC community at the JS site due to its weak reactivity in the
long-range transport.

585 One can see that air mass trajectories could be cluster into northern trajectories (Cluster 1 + 2), northeastern trajectory
(Cluster 3), southeastern trajectory (Cluster 4), southwestern trajectory (Cluster 5) and northwestern trajectory (Cluster 6) at
the PD site, as shown in Fig. 8b. It is evident that the contributions of northern (Cluster 1) and northeastern (Cluster 3)
trajectories to the total trajectories both the total trajectories and the total pollution trajectories were great higher than other
four cluster trajectories, accounting for 52.23 and 54.72 %, respectively. The results suggested that VOCs was significantly
590 influenced by the pollution transportation from East China Sea, Zhejiang Province and Jiangsu Province junction, as well as
local sources. The proportions of VOCs by each air mass trajectories indicated that alkanes and alkenes contributed to the
transported VOC community at the PD site.

At the QP site (Fig. 8c), the trajectories were clustered into the northern trajectories (Cluster 1 + 2), northeastern trajectory
(Cluster 3), southeastern trajectory (Cluster 4), southwestern trajectory (Cluster 5) and northwestern trajectory (Cluster 6).
595 The proportion of northeastern trajectory to both the total trajectories and the total pollution trajectories were higher than
those of the other trajectories, accounting for 31.87 and 27.81 %, respectively. This result indicated that the concentration of
VOCs was mainly impacted by the northeastern trajectory from the junction of East China Sea, Zhejiang Province and
Jiangsu Province in addition to local sources. Although the contribution of Cluster 2 was relatively small, the VOC
concentration was the highest, reaching 23.63 ± 10.75 ppb (Tab. 1). Therefore, attention should be paid to the long-distance
600 transmission of highly polluted from Beijing, Tianjin and Liaoning Province. The alkanes contributed most of VOCs in air
mass trajectories at the QP site, which was in line with the results of the JS site.

The region with high PSCF levels indicates highly potential regional transport sources (Hui et al., 2018). Based on the PSCF
results, at the JS and QP sites, high values were observed to the north of Shanghai, while at the PD site, high values were
observed to the northeast of Shanghai. All of the three sampling sites presented that the highest PSCF levels appeared around
605 the central area. Shanghai is the junction of economy, finance, trade and technology, there are a large number of local sources
such as vehicle emission, industrial source and fuel evaporation, which contributed most to the local VOC concentration,



610

indicating that local sources played an important role in the pollution of VOCs. Similarly, Song et al. (2021) studied the PSCF values at three different sites in Xi'an, China, and showed that Xi'an had a strong local source, which was also consistent with the findings in Wuhan, China (Hui et al., 2018; Hui et al, 2019), suggesting that local source was a significant contributor to the VOC pollution.

3.4 Secondary transformation potential

3.4.1 SOA formation potential

615

The close linkages between VOCs and particle formation induced the quantitative discussion on SOAFP (Chen et al., 2007; Guo et al., 2017; Tan et al., 2018), and the Grosjean's methodology has been widely recommended as the standard reference (Fig. 9). The SOAFP was calculated only for daytime (8:00-17:00 LT) to avoid the emission from the human activities during nighttime (Grosjean and Seinfeld, 1989; Zhang et al., 2020b). During the observation campaign, the SOAFP was averaged to be 1.00, 0.46 and 0.41 $\mu\text{g m}^{-3}$ at the JS, PD and QP sites, respectively. Such levels were comparable with those obtained in Jinan (Zhang et al., 2017) and Taiwan, China (Vo et al., 2018), while were higher than those of Nanjing, China (Mozaffar et al., 2020) (Tab. S2). The secondary potentials accounted for 2.19, 0.95 and 1.02 % of the $\text{PM}_{2.5}$ concentrations at the above sampling sites, all of which were lower than the results in Nanjing, China (3.46%) (Mozaffar et al., 2020) and Wangdu, China (8.4 and 17.84 % under high- NO_x and low- NO_x conditions) (Zhang et al., 2020b). Although the SOA contribution to $\text{PM}_{2.5}$ was low, the SOAFP values in the present study were underestimated. Only 21 VOC species were included in the estimations, and the VOC concentrations in the daytime were only 20.80, 9.43 and 7.30 ppb at the JS, PD and QP sites, respectively. Moreover, the published FAC values were obtained by merely considering the OH-related interactions, conservative estimations of the SOAFP values should be noted in the relevant research (de Gouw et al., 2011; Hennigan et al., 2011; Spracklen et al., 2011; Zhang et al., 2020b). Additionally, the discrepancies could also be induced by the different atmospheric conditions and study area. In the current study, the aromatics, such as BTEX, were determined to be the main SOA contributors, and the five compounds totally accounted for 86.07, 96.21 and 86.38 % at the JS, PD and QP sites, respectively, in accordance with the findings in Jinan, China (Zhang et al., 2017). Therefore, to achieve the better SOA reduction effects, the concentration of BTEX should be controlled in priority at the sampling sites, and more efficient strategies should be developed to limit the emissions of vehicle exhaust.

620

625

630

3.4.2 The VOCs- $\text{PM}_{2.5}$ sensitivity

635

The close associations between VOCs and SOA could induce the sensitive response of VOC concentrations to the different pollution degree of $\text{PM}_{2.5}$. In order to further understand the plausible influences on the atmospheric abundance of $\text{PM}_{2.5}$, the VOCs- $\text{PM}_{2.5}$ sensitivity ($\text{VOCs-S}_{\text{PM}_{2.5}}$) was applied to reduce the analysis error. Atmospheric pollution here can be divided into five levels by the mass concentration of $\text{PM}_{2.5}$: clean level ($\text{PM}_{2.5} < 35 \mu\text{g m}^{-3}$); slight pollution level ($35 < \text{PM}_{2.5} < 75 \mu\text{g m}^{-3}$); medium pollution level ($75 < \text{PM}_{2.5} < 120 \mu\text{g m}^{-3}$); heavy pollution level ($120 < \text{PM}_{2.5} < 180 \mu\text{g m}^{-3}$); extreme pollution



level ($PM_{2.5} > 180 \mu\text{g m}^{-3}$) (Han et al., 2017). The evolutions of VOCs- $S_{PM_{2.5}}$ as a function of $PM_{2.5}$ concentration at the JS, PD and QP sites are shown in Fig. 10. The low values of VOCs-S basically remain constant, while the high values displayed a descending trend. In the clean level, VOCs- $S_{PM_{2.5}}$ varied greatly from 0.19 to 2.50, 0.26 to 2.17 and 0.11 to 3.26 at the JS, PD and QP sites, respectively. In the pollution level, the scope of VOCs- $S_{PM_{2.5}}$ was narrow, especially in the extreme pollution level with the values fluctuating from 0.10 to 0.16, 0.13 to 0.17 and 0.17 to 0.28 at the JS, PD and QP sites, respectively. It is worth noting that the VOCs- $S_{PM_{2.5}}$ values displayed a steady decreasing trend, and the ratios of $PM_{2.5}$ values to $B_{PM_{2.5}}$ was increased in the clean and slight polluted levels. Such results demonstrated that the VOC concentrations were sensitive to that of $PM_{2.5}$ in the above two episodes. In order to quantify the sensitivity of VOCs to $PM_{2.5}$, we classified VOCs and $PM_{2.5}$ into different groups with a $PM_{2.5}$ concentration interval of $5 \mu\text{g m}^{-3}$, on the basis of the reported by Han et al. (2017). The mean VOCs- $S_{PM_{2.5}}$ values followed an exponential function, and the values of k were determined to be 0.39, 0.46 and 0.56 at the JS, PD and QP sites, respectively, according to the Eqs. (11-14). The VOCs at the QP site could be more sensitive to $PM_{2.5}$ relative to other two sites because greater k normally indicated the rapider increment of VOC concentrations. The four groups of VOCs displayed similar linkages with VOCs, and the higher values of k was attributed to the aromatics at the JS and PD sites, while the alkanes at the QP site (Fig. S6). Thus, the optimal choices of controlling VOC species presented difference at the diverse sampling sites. Accordingly, in order to efficiently control the VOC-induced haze pollution, the concentrations of aromatics at the JS and PD sites, as well as alkanes at the QP site should be controlled in priority, as the results of “clean-haze” discrepancy.

3.5 Photochemical reactivity of VOCs

3.5.1 Ozone formation potential

The atmospheric photochemical reactivity of VOCs makes them widely considered as the important precursors of O_3 (Alghamdi et al., 2014; Kumar et al., 2018). Hereby, the OFPs were calculated to be 50.89, 33.94 and 24.26 ppb at the JS, PD and QP sites, respectively (Fig. 11). Such secondary potentials accounted for 69.15, 59.05 and 24.43 % of the measured O_3 concentrations in the above sampling sites. Obviously, the contributions of VOCs to $PM_{2.5}$ (2.19, 0.95 and 1.02 % at the JS, PD and QP sites) were lower than those to O_3 at the sampling sites. The VOCs-related O_3 contributions were lower than those in Delhi, India (Kumar et al., 2018), and Chinese cities like Shanghai, China (Zhang et al., 2018a); Wuhan, China (Hui et al., 2018); Taiwan, China (Vo et al., 2018); Nanjing, China (Mozaffar et al., 2020); Xi’an, China (Song et al., 2021). The relatively low OFP could be explained by the slight VOC pollution during the sampling periods (Tab. S2). As the predominate contributor of OFP, alkenes category, especially the ethylene and propylene therein, presented great reactivity in atmospheric process and thus explains more than half of the photochemical reactivity at the three sampling sites, in line with the previous findings (An et al., 2014; Guo et al., 2017; Hui et al., 2018). Moreover, the considerable photochemical reactivity of aromatics (Li et al., 2019b), especially the toluene, *o*-xylene, *m/p*-xylene therein, makes them become the second largest contributor of OFP. Hence, alkenes and aromatics played a key role in the formation of O_3 and the relevant



670 emission sources, which are thought to be the industrial production and vehicle exhaust at the sampling sites, should be controlled in priority. By comparison, the fraction of aromatics at the JS site was higher than those at the PD and QP sites. The PD site showed high alkanes contribution compared with the JS and QP sites. In addition, the large contribution of alkenes was found at the QP site. Such phenomenon suggested that the OFP values were varied with the different land-use types. Therefore, it is necessary to study the OFP values at the varied site locations.

675 The OFPs of the VOC categories and O₃ concentration in March were suffered from the O₃ pollution reaching 93.13, 70.68 and 107.52 ppb at the JS, PD and QP sites, respectively (Fig. S5). It is worthwhile to note that, the relatively high VOC concentrations were observed at the JS and PD sites, resulting in the higher OFPs than that at the QP site. Under the high OFP (56.09 ± 37.73 and 45.53 ± 21.32 ppb), the concentration of O₃ at the JS and PD sites were unexpectedly lower than that at the QP site, indicating the unsatisfactory O₃ formation conditions, since the estimated OFP was proceeded within the optimum conditions. The highest concentration of O₃ was observed at the QP site, which was influenced by favorable meteorological conditions and possible external transportation. Such results were in good agreement with the findings in Zhengzhou, China (Li et al., 2019b).

3.5.2 The VOCs-O₃ sensitivity

It was well documented that O₃ formation was sensitive to the concentration of VOCs in many megacities along with high NO_x levels (Shao et al., 2009; Ou et al., 2016; Gao et al., 2017, Li et al., 2019b). To further examine the relationship between VOCs and O₃, the VOCs-SO₃ sensitivity (VOCs-SO₃) was used which was the similar method in analyzing the VOCs-SPM_{2.5} sensitivity. As discussed above, the O₃ concentrations were classified into clean level (O₃ < 110 μg m⁻³), slight pollution level (110 < O₃ < 120 μg m⁻³), medium pollution level (120 < O₃ < 130 μg m⁻³), heavy pollution level (130 < O₃ < 160 μg m⁻³), and extreme pollution level (O₃ > 160 μg m⁻³). The variations of VOCs-SO₃ at three sampling sites are shown in Fig. 12. The O₃ concentrations were more susceptible to the variation of low VOC concentrations than the high atmospheric abundance of VOCs. Therefore, more attention should be paid to the O₃ pollution and its evolutions during the clean and slight polluted periods. Besides, the lowest VOCs-SO₃ values were basically remain constant, while the high values showed the decreasing trends. To deeply understand the sensitivity of VOCs to O₃, the VOCs-SO₃ cases were subdivided into different groups with an O₃ concentration interval of 5 μg m⁻³. The results were varied with the sampling locations, i.e., at the JS site, the average values of VOCs-SO₃ in each group were fitted with an exponential function (Fig. 12):

$$y = 0.64 \cdot x^{-0.59}$$

The linear coefficient *k* was calculated to be 0.41 based on the Eqs. (11-14). At the PD site, the low and high values of VOCs-SO₃ fluctuated slightly, while the remained values increased along the O₃ gradient. At the QP site, the VOCs-SO₃ increased with elevated O₃ concentration while decreased. With regard to the four VOC categories, the high VOCs-SO₃ was primarily contributed from the alkenes and averaged to be 0.37, 0.40 and 0.52 at the JS, PD and QP, respectively (Fig. S7), which were agreed well with the OFP estimation results. The phenomenon suggested that the control measurements on



alkene emissions could provide direct insight into the issue of alleviating O₃ pollution at the sampling sites.

4. Conclusions

705 Herein, a concurrent atmospheric observation campaign was performed at the three supersites of Shanghai from January to March 2019. The sampling sites located at the industrial district (the Jinshan site: JS), residential district (the Pudong site: PD) and background district (the Qingpu site: QP) of Shanghai. Based on the observation data, this study has discussed in detail the pollution characteristics, primary sources and secondary pollution potentials of the atmospheric VOCs.

710 The mean VOC concentrations at the JS (21.39 ± 12.58 ppb) and PD (21.36 ± 8.58 ppb) sites were approximately twice higher than those at the QP site (11.93 ± 6.33 ppb). Alkanes dominated the VOC community and accounted for 50.33, 71.48 and 60.88 % of the VOCs at the JS, PD and QP sites, respectively. The diurnal variations showed the high VOC concentrations during the rush traffic hours in the morning and evening. However, the VOC concentrations on the weekends were 3.31, 10.19 and 1.19 % lower than those on the weekdays at the JS, PD and QP sites, respectively, due to the low anthropogenic activities occurring on the weekends. Overall, the VOC pollution characteristics varied with the sampling locations. The average PM_{2.5} values were 45.57 ± 27.59 , 48.51 ± 27.22 and 40.27 ± 27.78 $\mu\text{g m}^{-3}$ at the JS, PD and QP sites, respectively. The highest O₃ concentration was observed at the QP site (99.30 ± 24.00 ppb), followed by the JS (73.59 ± 23.59 ppb) and PD (57.48 ± 20.49 ppb) sites. The occurrence of haze pollution was characterized by the elevated concentrations of aromatics at the JS and PD sites, while the alkanes at the QP site.

720 The special ratios and PMF were used to investigate the local sources. Local anthropogenic emissions contributed largely to the VOC pollutions. The vehicle exhaust was determined as the predominate source at the three sites. The second largest VOC contributor was identified as industrial production at the JS and PD sites, while fuel evaporation was the second important source at the QP site. Apart from the local sources, the influence of regional transport was analyzed *via* 24-h back trajectories and PSCF. The results showed that VOCs were impacted by the north or/and northeast trajectories at three sampling sites. The highest PSCF values were observed in the area near the above sites, indicating that local source was a significant contributor to the VOC pollution.

725 The formation potentials of SOA and O₃ induced by the studied VOCs were also discussed. The results showed that VOCs had higher contribution to O₃ compared with PM_{2.5}, and the sensitivity analysis of VOC compositions varied with the sampling sites. Specifically, the SOAFP results illustrated that BTEX was the greatest contributor to SOAFP, comprising 86.07, 96.21 and 86.38 % at the JS, PD and QP sites, respectively. The VOCs-PM_{2.5} sensitivity analysis showed that VOCs at the QP site was more sensitive to PM_{2.5} compared with other two sampling sites. Of the four VOCs categories, aromatics at the JS and PD sites and alkanes at the QP site were more sensitive to PM_{2.5}. In terms of OFP, alkenes was the major OFP contributor, and meanwhile, aromatic compounds were also positively associated with the high OFP. The VOCs-O₃ sensitivity analysis showed that the VOCs-SO₃ values varied with sampling sites, and alkenes was more sensitive to O₃. The relevant results indicated that alkenes and aromatics were key concerns in reducing the atmospheric secondary pollution in



735 Shanghai. This study broadens the city-scale research from single-site measurement to multi-site observations, and simultaneously narrows the multi-site research from worldwide scale to city scale. The relevant results reveal the influences of land use type on atmospheric pollution, and set an example for the future VOC observation research.

Data availability

Measurement data in this study are available in the data repository maintained by Mendeley Data <https://doi.org/10.17632/mf4gf36r9n.1> (Han, 2022).

740 **Acknowledgements**

This work was supported by National Natural Science Foundation of China (Nos. 22176038, 91744205, 21777025).



References

- Ahmad, W., Coeur, C., Tomas, A., Fagniez, T., Brubach, J. B., and Cuisset, A.: Infrared spectroscopy of secondary organic aerosol precursors and investigation of the hygroscopicity of SOA formed from the OH reaction with guaiacol and syringol, *Appl. Optics.*, 56(11), E116, <https://doi.org/10.1364/AO.56.00E116>, 2017.
- Alghamdi, M. A., Khoder, M., Abdelmaksoud, A. S., Harrison, R. M., Hussein, T., Lihavainen, H., and Hämeri, K.: Seasonal and diurnal variations of BTEX and their potential for ozone formation in the urban background atmosphere of the coastal city Jeddah, Saudi Arabia, *Air Qual. Atmos. Health* 7(4), 467-480. <https://doi.org/10.1007/s11869-014-0263-x>, 2014.
- Amor-Carro, O., White, K. M., Fraga-Iriso, R., Marinas-Pardo, L. A., Nunez-Naveira, L., Lema-Costa, B., Villarnovo, M., Vereza-Hernando, H., and Ramos-Barbon, D.: Airway hyperresponsiveness, inflammation, and pulmonary emphysema in rodent models designed to mimic exposure to fuel oil-derived volatile organic compounds encountered during an experimental oil spill, *Environ. Health Persp.* 128: 027003, 1-14, <https://doi.org/10.1289/EHP4178>, 2020.
- An, J., Zhu, B., Wang, H., Li, Y., Lin, X., and Yang, H.: Characteristics and source apportionment of VOCs measured in an industrial area of Nanjing, Yangtze River Delta, China, *Atmos. Environ.*, 97, 206-214, <https://doi.org/10.1016/j.atmosenv.2014.08.021>, 2014.
- An, J. L., Wang, J. X., Zhang, Y. X., and Zhu, B.: Source Apportionment of Volatile Organic Compounds in an Urban Environment at the Yangtze River Delta, China, *Arch. Environ. Con. Tox.*, 72(3), 335-348, <https://doi.org/10.1007/s00244-017-0371-3>, 2017.
- Ashbaugh, L. L., Malm, W. C., Sadeh, W. Z. A residence time probability analysis of sulfur concentrations at ground canyon national park, *Atmos. Environ.*, 19(8), 1263-1270, [https://doi.org/10.1016/0004-6981\(85\)90256-2](https://doi.org/10.1016/0004-6981(85)90256-2), 1985.
- Atkinson, R. and Arey, J.: Gas-phase tropospheric chemistry of biogenic volatile organic compounds: a review, *Atmos. Environ.*, 2, 37, [https://doi.org/10.1016/S1352-2310\(03\)00391-1](https://doi.org/10.1016/S1352-2310(03)00391-1), 2003.
- Bari, M. A. and Kindziarski, W. B.: Ambient volatile organic compounds (VOCs) in Calgary, Alberta: Sources and screening health risk assessment, *Sci. Total Environ.*, 631-632, 627-640, <https://doi.org/10.1016/j.scitotenv.2018.03.023>, 2018.
- Brown, S. G., Eberly, S., Paatero, P., Norris, and G. A.: Methods for estimating uncertainty in PMF solutions: Examples with ambient air and water quality data and guidance on reporting PMF results, *Sci. Total Environ.*, 518-519, 626-635, <https://doi.org/10.1016/j.scitotenv.2015.01.022>, 2015.
- Brown, S. G., Frankel, A., and Hafner, H. R.: Source apportionment of VOCs in the Los Angeles area using positive matrix factorization, *Atmos. Environ.*, 41, 227-237, <https://doi.org/10.1016/j.atmosenv.2006.08.021>, 2007.
- Cai, C., Geng, F., Yu, Q., An, J., Han, J.: Source apportionment of VOCs at city centre of Shanghai in summer, *Acta Sci. Circumst.*, 30 (5), 926-934, <https://doi.org/10.1631/jzus.A1000244>, 2010a
- Cai, C., Geng, F. H., Tie, X. X., Yu, Q., and An, J. L., Characteristics of ambient volatile organic compounds (VOCs) measured in Shanghai, China, *Sensors*, 10, 7843-7862, doi:10.3390/s100807843, 2010b.
- Calfapietra, C., Fares, S., and Lofeto, F: Volatile organic compounds from Italian vegetation and their interaction with ozone, *Environ. Pollut.*, 157(5), 1478-1486, <https://doi.org/10.1016/j.envpol.2008.09.048>, 2009.
- Carter, W. P. L.: Development of ozone reactivity scales for volatile organic compounds, *J. Air Waste Manage. Assoc.*, 44(7), 881-899, <https://doi.org/10.1080/1073161X.1994.10467290>, 1994.
- Chang, C. C., Wang, J. L., Liu, S. C., and Candice, L. S. C.: Assessment of vehicular and non-vehicular contributions to hydrocarbons using exclusive vehicular indicators, *Atmos. Environ.*, 40, 6349-6361, <https://doi.org/10.1016/j.atmosenv.2006.05.043>, 2006.
- Chen, T. M., Kuschner, W. G., Gokhale, J., and Schofer, S.: Outdoor air pollution: Ozone health effects, *Am. J. Med. Sci.*, 333(4), 244-248, <https://doi.org/10.1097/MAJ.0b013e31803b8e8c>, 2007.
- Chen, X., Millet, D. B., Singh, H. B., Wisthaler, A., Apel, E. C., Atlas, E. L., Blake, D. R., Bourgeois, I., Brown, S. S., Crounse, J. D., de Gouw, J. A., Flocke, F. M., Fried, A., Heikes, B. G., Hornbrook, R. S., Mikoviny, T., Min, K. E., Müller, M., Neuman, J. A., O'Sullivan, D. W., Peischl, J., Pfister, G. G., Richter, D., Roberts, J. M., Ryerson, T. B., Shertz, S. R., Thompson, C. R., Treadaway, V., Veres, P. R., Walega, J., Warneke, C., Washenfelder, R. A., Weibring, P., and Yuan, B.: On the sources and sinks of atmospheric VOCs: an integrated analysis of recent aircraft campaigns over North America, *Atmos. Chem. Phys.*, 19(14), 9097-9123, doi:10.5194/acp-19-9097-2019, 2019.
- Dai, H. X., Jing, S. G., Wang, H. L., Ma, Y. G., Li, L., Song, W. M., and Kan, H. D., VOC characteristics and inhalation



- health risks in newly renovated residences in Shanghai, China, *Sci. Total Environ.*, 577, 73-83, <https://doi.org/10.1016/j.scitotenv.2016.10.071>, 2017.
- Dai, P., Ge, Y., Lin, Y., Su, S., and Liang, B.: Investigation on characteristics of exhaust and evaporative emissions from passenger cars fueled with gasoline/methanol blends, *Fuel*. 2013, 113, 10-16, <https://doi.org/10.1016/j.fuel.2013.05.038>, 2013.
- de Gouw, J. A., Middlebrook, A. M., Warneke, C., Ahmadov, R., Atlas, E. L., and Bahreini, R.: Organic aerosol formation downwind from the Deeperwater Horizon oil spil, *Science* 331, 1295-1299, <https://doi.org/10.1126/science.1200320>, 2011.
- Debevec, C. Sauvage, S., Gros, V., Salameh, T. Sciare, J., Dulac, F., and Locoge, N.: Seasonal variation and origins of volatile organic compounds observed during 2 years at a western Mediterranean remote background site (Ersa, Cape Corsica), *Atmos. Chem. Phys.*, 21, 1449-1484, <https://doi.org/10.5194/acp-21-1449-2021>, 2021.
- Dechapanya, W., Eusebi, A., Kimura, Y., and Allen, D. T.: Secondary organic aerosol formation from aromatic precursors. 1. Mechanisms for individual hydrocarbons, *Environ. Sci. Technol.*, 37, 3662-3670, <https://doi.org/10.1021/es0209058>, 2003a
- Dechapanya, W., Eusebi, A., Kimura, Y., and Allen, D. T.: Secondary organic aerosol formation from aromatic precursors. 2. Mechanisms for lumped aromatic hydrocarbons, *Environ. Sci. Technol.* 37, 3671-3679, <https://doi.org/10.1021/es0209060>, 2003b.
- Deng, C. X., Jin, Y. J., Zhang, M., Liu, X. W., and Yu, Z. M.: Emission Characteristics of VOCs from On-Road Vehicles in an Urban Tunnel in Eastern China and Predictions for 2017-2026, *Aerosol Air Qual. Res.*, 18, 3025-3034, <https://doi.org/10.4209/aaqr.2018.07.0248>, 2018.
- Draxier, R. R., and Hess, G. D.: An overview of the hysplit-4 modelling system for trajectories, *Aust. Meteorol. Mag.*, 1998, 47(4), 295-308.
- Dumanoglu, Y., Kara, M., Altiok, H., Odabasi, M., Elbir, T. and Bayram, A.: Spatial and seasonal variation and source apportionment of volatile organic compounds (VOCs) in a heavily industrialized region, *Atmos. Environ.*, 98, 168-178, <https://doi.org/10.1016/j.atmosenv.2014.08.048>, 2014.
- Gao, W., Tie, X., Xu, J., Huang, R., Mao, X., Zhou, G., and Chang, L.: Long-term trend of O₃ in a mega City 694 (Shanghai), China: Characteristics, causes, and interactions with precursors, *Sci. Total Environ.*, 695 603-604, <https://doi.org/10.1016/j.scitotenv.2017.06.099>, 2017
- Gaimoz, C., Sauvage, S., Gros, V., Herrmann, F., Williams, J., Locoge, N., Perrussel, O., Bonsang, B., d'Argouges, O., Sarda-Estève, R., and Sciare, J.: Volatile organic compounds sources in Paris in spring 2007. Part II: Source apportionment using positive matrix factorisation, *Environ. Chem.*, 8, 91-103, <https://doi.org/10.1071/EN10067>, 2011.
- Geng, F. H., Cai, C. J., Tie, X. X., Yu, Q., An, J. L., Peng, L., Zhou, G. Q., and Xu, J. M.: Analysis of VOC emissions using PCA/APCS receptor model at city of Shanghai, China, *J. Atmos. Chem.*, 62(3), 229-247, <https://doi.org/10.1007/s10874-010-9150-5>, 2009.
- Geng, F. H., Tie, X. X., Xu, J. M., Zhou, G. Q., Peng, L., Gao, W., Tang, X., and Zhao, C. S.: Characterizations of ozone, NO_x, and VOCs measured in Shanghai, China, *Atmos. Environ.*, 42, 6873-6883, doi:10.1016/j.atmosenv.2008.05.045, 2008.
- Grosjean, D. and Seinfeld, J. H.: Parameterization of the formation potential of secondary organic aerosols., *Atmos. Environ.*, 23(8), 1733-1747, [https://doi.org/10.1016/0004-6981\(89\)90058-9](https://doi.org/10.1016/0004-6981(89)90058-9), 1989.
- Guenther, A., Hewitt, C. N., Erickson, D., Fall, R., Geron, C., Graedel, T., Harley, P., Klinger, L., Lerdau, M., Mckay, W. A., Pierce, T., Scholes, B., Steinbrecher, R., Tallamraju, R., Taylor, J., and Zimmerman, P.: A global-model of natural volatile organic-compound emissions, *J. Geophys. Res-A.*, 100, 8873-8892, <https://doi.org/10.1029/94JD02950>, 1995.
- Guo, H., Cheng, H. R., Ling, Z. H., Louie, P. K. K., and Ayoko, G. A.: Which emission sources are responsible for the volatile organic compounds in the atmosphere of Pearl River Delta?, *J. Hazard. Mater.*, 188(1-3), 116-124, <https://doi.org/10.1016/j.jhazmat.2011.01.081>, 2011.
- Guo, H., Ling, Z. H., Cheng, H. R., Simpson, I. J., Lyu, X. P., Wang, X. M., Shao, M. Z., Lu, H. X., Ayoko, G., Zhang, Y. L., Saunders, S., Lam, S., Wang, J. L., and Blake, D. R.: Tropospheric volatile organic compounds in China, *Sci. Total Environ.*, 574, 1021-1043, <https://doi.org/10.1016/j.scitotenv.2016.09.116>, 2017.
- Guo, H., Wang, T., and Louie, P. K.: Source apportionment of ambient non-methane hydrocarbons in Hong Kong: application of a principal component analysis/absolute principal component scores (PCA/APCS) receptor model,



- Environ. Pollut., 129 (3), 489-498, <https://doi.org/10.1016/j.envpol.2003.11.006>, 2004.
- Han, D. M., Wang, Z., Cheng, J. P., Wang, Q., Chen, X. J., and Wang, H. L.: Volatile organic compounds (VOCs) during non-haze and haze days in Shanghai: characterization and secondary organic aerosol (SOA) formation, *Environ. Sci. Pollut. Res.*, 24, 18619-18629, <https://doi.org/10.1007/s11356-017-9433-3>, 2017.
- Han, M., Lu, X. Q., Ran, L., Zhao, C. S., Han, S. Q., Bao, J. L., Zou, K. H., and Yan, F. Y.: Source apportionment of volatile organic compounds in urban Tianjin in the summer, *Chin. Environ. Sci. Technol.*, 34(10), 76-80, <https://doi.org/10.3969/j.issn.1003-6504.2011.10.017>, 2011.
- Han, Y.: Data for: "Measurement report: Simultaneous multi-site observations of VOCs in Shanghai, East China: characteristics, sources and secondary formation potentials", Mendeley Data [data set], <https://doi.org/10.17632/mf4gf36r9n.1>, 2022.
- He, Z. R., Wang, X. M., Ling, Z. H., Zhao, J., Guo, H., Shao, M., and Wang, Z.: Contributions of different anthropogenic volatile organic compound sources to ozone formation at a receptor site in the Pearl River Delta region and its policy implications, *Atmos. Chem. Phys.*, 19(13), 8801-8816, <https://doi.org/10.5194/acp-19-8801-2019>, 2019.
- Heald, C. L., Gouw, J. De, Goldstein, A. H., Guenther, A. B., Hayes, P. L., Hu, W., Isaacman-Vanwertz, G., Jimenez, J. L., Keutsch, F. N., Koss, A. R., Misztal, P. K., Rappenglück, B., Roberts, J. M., Stevens P. S., Washenfelder, R. A., Warneke, C., and Young, C. J.: Contrasting reactive organic carbon observations in the Southeast United States (SOAS) and Southern California (CalNex), *Environ. Sci. Technol.*, 54(23), 14923-14935, <https://doi.org/10.1021/acs.est.0c05027>, 2020.
- Hennigan, C. J., Miracolo, M. A., Engelhart, G. J., May, A. A., Presto, A. A., Lee, T., Sullivan, A. P., Mucmeking, G., Coe, H., Wold, C. E., Hao, W. M., Gilman, J. B., Kuster, W. C., Gouw, J. D., Schichtel, B., Collett-Jr, J. L., Kreidenweis, S. M., and Robinson, E. S.: Chemical and physical transformations of organic aerosol from the photo-oxidation of open biomass burning emissions in an environmental chamber, *Atmos. Chem. Phys.*, 11, 7669-7686, <https://doi.org/10.5194/acpd-11-11995-2011>, 2011.
- Hong, Z., Li, M., Wang, H., Xu, L., Hong, Y., Chen, J., Chen, J., Zhang, H., Zhang, Y., Wu, X., Hu, B., and Li, M.: Characteristics of atmospheric volatile organic compounds (VOCs) at a mountainous forest site and two urban sites in the southeast of China, *Sci. Total Environ.*, 657, 1491-1500, <https://doi.org/10.1016/j.scitotenv.2018.12.132>, 2019.
- Hoshi, J., Amano, S., Sasaki, Y., and Korenaga, T.: Investigation and estimation of emission sources of 54 volatile organic compounds in ambient air in Tokyo, *Atmos. Environ.*, 42(10), 2383-2393, <https://doi.org/10.1016/j.atmosenv.2007.12.024>, 2008.
- Hopke, P. K. Review of receptor modeling methods for source apportionment, *J. Air Waste Manage. Assoc.*, 66(3), 237-259, <https://doi.org/10.1080/10962247.2016.1140693>, 2016.
- Huang, C., Wang, H. L., Li, L., Wang, Q., Lu, Q., de Gouw, J. A., Zhou, M., Jing, S. A., Lu, J., and Chen, C. H.: VOC species and emission inventory from vehicles and their SOA formation potentials estimation in Shanghai, China, *Atmos. Chem. Phys.*, 15, 11081-11096, <https://doi.org/10.5194/acp-15-11081-2015>, 2015.
- Huang, R. J., Zhang, Y., Bozzetti, C., Ho, K. F., Cao, J. J., Han, Y. M., Daellenbach, K. R., Slowik, J. G., Platt, S. M., Canonaco, F., Zotter, P., Wolf, R., Pieber, S. M., Bruns, E. A., Crippa, M., Ciarelli, G., Piazzalunga, A., Schwikowski, M., Abbazade, G., Schnelle-Kreis, J., Zimmermann, R., An, Z., Szidat, S., Baltensperger, U., Haddad, I. E., and Prévôt, A. S. H.: High secondary aerosol contribution to particulate pollution during haze events in China, *Nature*, 514, 218-222, <https://doi.org/10.1038/nature13774>, 2014.
- Hui, L. R., Liu, X. G., Tan, Q. W., Feng, M., An, J. L., Qu, Y., Zhang Y. H., and Cheng, N. L.: VOC characteristics, sources and contributions to SOA formation during haze events in Wuhan, Central China, *Sci. Total Environ.*, 650, 2624-2639, <https://doi.org/10.1016/j.scitotenv.2018.10.029>, 2019.
- Hui, L. R., Liu, X. G., Tan, Q. W., Feng, M., An, J. L., Qu, Y., Zhang, Y. H., and Jiang, M. Q.: Characteristics, source apportionment and contribution of VOCs to ozone formation in Wuhan, Central China, *Atmos. Environ.*, 192, 55-71, <https://doi.org/10.1016/j.atmosenv.2018.08.042>, 2018.
- Jobson, B. T., Parrish, D. D., Goldan, P., Kuster, W., Fehsenfeld, F. C., Blake, D. R., and Niki, H.: Spatial and temporal variability of nonmethane hydrocarbon mixing ratios and their relation to photochemical lifetime, *J. Geophys. Res. Atmos.*, 103(D11), 13557-13567, <https://doi.org/10.1029/97JD01715>, 1998.
- Kumar, A., Singh, D., Kumar, K. S., Singh, B. B., and Jain, V. K.: Distribution of VOCs in urban and rural atmospheres of subtropical India: Temporal variation, source attribution, ratios, OFP and risk assessment, *Sci. Total Environ.*, 613-614,



- 492-501, <https://doi.org/10.1016/j.scitotenv.2017.09.096>, 2018.
- Lai, C., Chuang, K., and Chang, J.: Source apportionment of volatile organic compounds at an international airport, *Aerosol Air Qual. Res.*, 13, 689-698, <https://doi.org/10.4209/aaqr.2012.05.0121>, 2013.
- Lam, S. H. M., Saunders, S. M., Guo, H., Ling, Z. H., Jiang, F., Wang, X. M., and Wang, T. J.: Modelling VOC source impacts on high ozone episode days observed at a mountain summit in Hong Kong under the influence of mountain-valley breezes, *Atmos. Environ.*, 81(2), 166-176, <https://doi.org/10.1016/j.atmosenv.2013.08.060>, 2013.
- Li, B., Ho, S. S. H., Gong, S., Ni, J., Li, H., Han, L., Yang, Y., Qi, Y., and Zhao, D.: Characterization of VOCs and their related atmospheric processes in a central Chinese city during severe ozone pollution period, *Atmos. Chem. Phys.*, 9(1), 617-638, <https://doi.org/10.5194/acp-19-617-2019>, 2019b.
- Li, J., Xie, S. D., Zeng, L. M., Li, L. Y., Li, Y. Q., and Wu, R. R.: Characterization of ambient volatile organic compounds and their sources in Beijing, before, during, and after Asia-Pacific Economic Cooperation China 2014, *Atmos. Chem. Phys.*, 15(14), 7945-7959, <https://doi.org/10.5194/acp-15-7945-2015>, 2015a.
- Li, J., Zhai, C. Z., Yu, J. Y., Liu, R. L., Li, Y. Q., Zeng, L. M., and Xie, S. D.: Spatiotemporal variations of ambient volatile organic compounds and their sources in Chongqing, a mountainous megacity in China, *Sci. Total Environ.*, 627, 1442-1452, <https://doi.org/10.1016/j.scitotenv.2018.02.010>, 2018.
- Li, L., Tan, Q., Zhang, Y., Feng, M., Qu, Y., An, J., and Liu, X.: Characteristics and source apportionment of PM_{2.5} during persistent extreme haze events in Chengdu, Southwest China, *Environ. Pollut.*, 230, 718-729, <https://doi.org/10.1016/j.envpol.2017.07.029>, 2017.
- Li, L., Xie, S., Zeng, L., Wu, R., and Li, J.: Characteristics of volatile organic compounds and their role in ground-level ozone formation in the Beijing-Tianjin-Hebei region, China, *Atmos. Environ.*, 113, 247-254, <https://doi.org/10.1016/j.atmosenv.2015.05.021>, 2015b.
- Li, M., Zhang, Q., Zheng, B., Tong, D., Lei, Y., Liu, F., Hong, C., Kang, S., Yan, L., Zhang, Y., Bo, Y., Su, H., Cheng, Y., and He, K.: Persistent growth of anthropogenic non-methane volatile organic compound (NMVOC) emissions in China during 1990-2017: drivers, speciation and ozone formation potential, *Atmos. Chem. Phys.*, 19, 8897-8913, <https://doi.org/10.5194/acp-19-8897-2019>, 2019a.
- Li, X. H., Wang, S. X., and Hao, J. M.: Characteristics of Volatile Organic Compounds (VOCs) Emitted from Biofuel Combustion in China, *Environ. Sci.*, 32, 3515-3521, <https://doi.org/10.1109/ICMTMA.2014.201>, 2011.
- Li, Y. J., Ren, B. N., Qiao, Z., Zhu, J. P., Wang, H. L., Zhou, M., Qiao, L. P., Lou, S. R., Jing, S. G., Huang, C., Tao, S. K., Rao, P. H., and Li, J.: Characteristics of atmospheric intermediate volatility organic compounds (IVOCs) in winter and summer under different air pollution levels, *Atmos. Environ.*, 210, 58-65, <https://doi.org/10.1016/j.atmosenv.2019.04.041>, 2019c.
- Li, Y. Q., Li, J., Wu, R. R., and Xie, S. D.: Characterization and source identification of ambient volatile organic compounds (VOCs) in a heavy pollution episode in Beijing, China, 207, 249-259, <https://doi.org/10.2495/AIR160231>, 2016.
- Li, Z. Y., Ho, K. F., and Yin, S. H. L.: Source apportionment of hourly-resolved ambient volatile organic compounds: Influence of temporal resolution, *Sci. Total Environ.*, 725, 138243, <https://doi.org/10.1016/j.scitotenv.2020.138243>, 2020.
- Ling, Z. H., Guo, H., Cheng, H. R., and Yu, Y. F.: Sources of ambient volatile organic compounds and their contributions to photochemical ozone formation at a site in the Pearl River Delta, southern China, *Environ. Pollut.*, 159 (10), 2310-2319, <https://doi.org/10.1016/j.envpol.2011.05.001>, 2011.
- Liu, S. C.: Ozone production in the rural troposphere and the implications for regional and global ozone distributions., *J. Geophys. Res.*, 92(D4), 4191-4207, <https://doi.org/10.1029/JD092iD04p04191>, 1987.
- Liu, Y., Shao, M., Fu, L. L., Lu, S. H., Zeng, L. M., and Tang, D. G.: Source profiles of volatile organic compounds (VOCs) measured in China: Part I, *Atmos. Environ.*, 42(25), 6247-6260. <https://doi.org/10.1016/j.atmosenv.2008>.
- Liu, Y., Song, M., Liu, X., Zhang, Y., Hui, L., Kong, L., Zhang, Y., Zhang, C., Qu, Y., An, J., Ma, D., Tan, Q., and Feng, M.: Characterization and sources of volatile organic compounds (VOCs) and their related changes during ozone pollution days in 2016 in Beijing, China, *Environ. Pollut.*, 257, 113599, 1-12, <https://doi.org/10.1016/j.envpol.2019.113599>, 2020.
- Liu, Y., Wang, H., Jing, S., Gao, Y., Peng, Y., Lou, S., Cheng, T., Tao, S., Li, L., Li, Y., Huang, D., Wang, Q., and An, J.: Characteristics and sources of volatile organic compounds (VOCs) in Shanghai during summer: Implications of regional transport, *Atmos. Environ.*, 215, 116902, 1-14, <https://doi.org/10.1016/j.atmosenv.2019.116902>, 2019.



- Liu, Y. H., Wang, H. L., Jing, S. G., Peng, Y. R., Gao, Y. Q., Yan, R. S., Wang, Q., Lou, S. R., Cheng, T. T., and Huang, C.: Strong regional transport of volatile organic compounds (VOCs) during wintertime in Shanghai megacity of China, *Atmos. Environ.*, 244, 117940, <https://doi.org/10.1016/j.atmosenv.2020.117940>, 2021.
- Lu, X., Hong, J., Zhang, L., Cooper, O. R., Schultz, M. G., Xu, X., Wang, T., Gao, M., Zhao, Y., and Zhang, Y.: Severe surface ozone pollution in China: A global perspective, *Environ. Sci. Technol. Lett.*, 5, 487-494, <https://doi.org/10.1021/acs.estlett.8b00366>, 2018.
- Lyu, X. P., Chen, N., Guo, H., Zhang, W. H., Wang, N., Wang, Y., and Liu, M.: Ambient volatile organic compounds and their effect on ozone production in Wuhan, Central China, *Sci. Total Environ.*, 541, 662-669, <https://doi.org/10.1016/j.scitotenv.2015.09.093>, 2016.
- Ma, T., Duan, F., He, K., Qin, Y., Tong, D., Geng, G., Liu, X., Li, H., Yang, S., Ye, S., Xu, B., Zhang, Q., and Ma, Y.: Air pollution characteristics and their relationship with emissions and meteorology in the Yangtze River Delta region during 2014-2016, *J. Environ. Sci.*, 83, 8-20, <https://doi.org/10.1016/j.jes.2019.02.031>, 2019.
- Mo, Z., Shao, M., Lu, S., Qu, H., Zhou, M., Sun, J., and Gou, B.: Process-specific emission characteristics of volatile organic compounds (VOCs) from petrochemical facilities in the Yangtze River Delta, China, *Sci. Total Environ.*, 533, 422-431, <https://doi.org/10.1016/j.scitotenv.2015.06.089>, 2015.
- Mo, Z., Shao, M., Lu, S.: Compilation of a source profile database for hydrocarbon and OVOC emissions in China, *Atmos. Environ.*, 143, 209-217, <https://doi.org/10.1016/j.atmosenv.2016.08.025>, 2016.
- Monod, A., Sive, B. C., Avino, P., Chen, T., Blake, D. R., and Rowland, F. S.: Monoaromatic compounds in ambient air of various cities: a focus on correlations between the xylenes and ethylbenzene, *Atmos. Environ.*, 35, 135-149, [https://doi.org/10.1016/S1352-2310\(00\)00274-0](https://doi.org/10.1016/S1352-2310(00)00274-0), 2001.
- Mousavinezhad, S., Choi, Y., Pouyaei, A., Ghahremanloo, M. and Nelson, D. L.: A comprehensive investigation of surface ozone pollution in China, 2015-2019: Separating the contributions from meteorology and precursor emissions, *Atmos. Res.*, 257, 105599, <https://doi.org/10.1016/j.atmosres.2021.105599>, 2021.
- Morrow, N.L.: The industrial production and use of 1,3-butadiene, *Environ. Health Perspect.*, 86, 7-8, <https://doi.org/10.1289/ehp.90867>, 1990.
- Mozaffar, A., Zhang, Y. L., Fan, M. Y., Cao, F., and Lin, Y. C.: Characteristics of summertime ambient VOCs and their contributions to O₃ and SOA formation in a suburban area of Nanjing, China, *Atmos. Res.*, 240, 104923, 1-16, <https://doi.org/10.1016/j.atmosres.2020.104923>, 2020.
- Murphy, J. G., Day, D. A., Cleary, P. A., Wooldridge, P. J., Millet, D. B., Goldstein, A. H., and Cohen, R. C.: The weekend effect within and downwind of Sacramento-Part I: Observation of ozone, nitrogen oxides, and VOC reactivity, *Atmos. Chem. Phys.*, 7(20): 5237-5339, <https://doi.org/10.5194/acp-7-5327-2007>, 2007.
- Nan, S. Q., Liang, J., Zhang, D., Zhang, R. Q., Jiang, N., Duo, K. X., and Zhang, J.: VOCs in ambient air of Zhengzhou City: spatial distribution and source apportionment, *China Environ. Sci. Technol.*, 38(3), 119-124, <https://doi.org/10.3969/j.issn.1003-6504.2015.03.023>, 2015.
- Nelson, P., and Quigley, S.: The m, p-xylenes: ethylbenzene ratio. A technique for estimating hydrocarbon age in ambient atmospheres, *Atmos. Environ.*, 17, 659-662, [https://doi.org/10.1016/0004-6981\(83\)90141-5](https://doi.org/10.1016/0004-6981(83)90141-5), 1983.
- Ng, N. L., Kroll, J. H., Chan, A. W. H., Chhabra, P. S., Flagan, R. C., and Seinfeld, J. H.: Secondary organic aerosol formation from m-xylene, toluene, and benzene, *Atmos. Chem. Phys.*, 7(14), 3909-3922, <https://doi.org/10.5194/acp-7-3909-2007>, 2007.
- Niu, H., Mo, Z., Shao, M., Lu, S., and Xie, S.: Screening the emission sources of volatile organic compounds (VOCs) in China by multi-effects evaluation, *Front. Env. Sci. Eng.*, 10(5), 1-11, <https://doi.org/10.1007/s11783-016-0828-z>, 2016.
- Nussbaumer, C. M. and Cohen, R. C.: The role of temperature and NO_x in ozone trends in the Los Angeles Basin, *Environ. Sci. Technol.*, 54, 15652-15659, <https://doi.org/10.1021/acs.est.0c04910>, 2020.
- Odum, J. R., Jungkamp, T. P. W., Griffin, R. J., Forstner, H. J. L., Flagan, R. C., and Seinfeld, J. H.: Aromatics, reformulated gasoline, and atmospheric organic aerosol formation, *Environ. Sci. Technol.*, 31(7), 1890-1897, <https://doi.org/10.1021/es960535l>, 1997.
- Ou, J., Yuan, Z., Zheng, J., Huang, Z., Shao, M., Li, Z., Huang, X., Guo, H., and Louie, P. K.: Ambient Ozone 810 Control in a Photochemically Active Region: Short-Term Despiking or Long-Term Attainment?, *Environ. Sci. Tech.*, 50, 5720-5728, <https://doi.org/10.1021/acs.est.6b00345>, 2016.



- Paatero, P.: Least squares formulation of robust non-negative factor analysis, *Chemom. Intell. Lab. Syst.*, 37(1), 23-35, [https://doi.org/10.1016/S0169-7439\(96\)00044-5](https://doi.org/10.1016/S0169-7439(96)00044-5), 1997.
- Pakkattil, A., Muhsin, M., and Varma, M. K. R.: COVID-19 lockdown: Effect on selected volatile organic compound (VOC) emissions over the major Indian metro cities, 37, 100838, <https://doi.org/10.1016/j.uclim.2021.100838>, 2021.
- Pallavi, Sinha, B., and Sinha, V.: Source apportionment of volatile organic compounds in the northwest Indo-Gangetic Plain using a positive matrix factorization model, *Atmos. Chem. Phys.*, 19(24), 15467-15482, <https://doi.org/10.5194/acp-19-15467-2019>, 2019.
- Pankow, J. F.: An absorption-model of gas-particle partitioning of organic-compounds in the atmosphere, *Atmos. Environ.*, 28, 185-188, [https://doi.org/10.1016/1352-2310\(94\)90093-0](https://doi.org/10.1016/1352-2310(94)90093-0), 1994.
- Polissar, A. V., Hopke, P. K., Paatero, P., Kaufmann, Y. J., Hall, D. K., Bodhaine, B. A., Dutton, E. G., and Harris, J. M.: The aerosol at Barrow, Alaska: long-term trends and source locations, *Atmos. Environ.*, 33, 2441-2458, [https://doi.org/10.1016/S1352-2310\(98\)00423-3](https://doi.org/10.1016/S1352-2310(98)00423-3), 1999.
- Ren, B. N., Zhu, J. P., Tian, L. J., Wang, H. L., Huang, C., Jing, S. A., Lou, S. G., An, J. Y., Lu, J., Rao, P. H., Fu, Q. Y., Huo, J. T., and Li, Y. J.: An alternative semi-quantitative GC/MS method to estimate levels of airborne intermediate volatile organic compounds (IVOCs) in ambient air, *Atmos. Environ.*, 6, 100075, <https://doi.org/10.1016/j.aeaoa.2020.100075>, 2020.
- Rumchev, K., Brown, H., and Spickett, J.: Volatile organic compounds: do they present a risk to our health?, *Rev. Environ. Health*, 22(1), 39-55, <https://doi.org/10.1515/REVEH.2007.22.1.39>, 2007.
- Sadeghi, B., Pouyaei, A., Choi, Y. S., and Rappenglueck, B. H.: Measurement report: Summertime and wintertime VOCs in Houston: Source apportionment and spatial distribution of source origins, *Atmos. Chem. Phys. Discussion*, 2021, 565, 1-27, <https://doi.org/10.5194/acp-2021-565>, 2021.
- Sawvel, E. J., Willis, R., West, R. R., Casuccio, G. S., Norris, G., Kumar, N., Hammond, D., and Peters, T. M.: Passive sampling to capture the spatial variability of coarse particles by composition in Cleveland, OH, *Atmos. Environ.*, 105, 61-69, <https://doi.org/10.1016/j.atmosenv.2015.01.030>, 2015.
- Seinfeld, J. H., Erdakos, G. B., Asher, W. E., and Pankow, J. F.: Modeling the formation of secondary organic aerosol (SOA). 2. The predicted effects of relative humidity on aerosol formation in the α -pinene-, β -pinene-, sabinene-, Δ 3-carene-, and cyclohexene-ozone systems. *Environ. Sci. Technol.*, 35, 1806-1817, <https://doi.org/10.1021/es011025g>, 2001.
- Schwantes, R. H., Schilling, K. A., Mcvay, R. C., Lignell, H., and Seinfeld, J. H.: Formation of highly oxygenated low-volatility products from cresol oxidation, *Atmos. Chem. Phys.*, 17(5), 1-34, <https://doi.org/10.5194/acp-17-3453-2017>, 2016.
- Shao, M., Lu, S., Liu, Y., Xie, X., Chang, C., Huang, S., and Chen, Z.: Volatile organic compounds measured in summer in Beijing and their role in ground-level ozone formation, *J. Geophys. Res.*, 114, 833, <https://doi.org/10.1029/2008jd010863>, 2009.
- Shao, P., An, J. L., Xin, J. Y., Wu, F. K., Wang, J. X., Ji, D. S., and Wang, Y. S.: Source apportionment of VOCs and the contribution to photochemical ozone formation during summer in the typical industrial area in the Yangtze River Delta, China, *Atmos. Res.*, s176-s177, 64-74, <https://doi.org/10.1016/j.atmosres.2016.02.015>, 2016.
- Shi, J., Deng, H., Bai, Z., Kong, S., Wang, X., Hao, J., Han, X., and Ning, P.: Emission and profile characteristic of volatile organic compounds emitted from coke production, iron smelt, heating station and power plant in Liaoning Province, China, *Sci. Total Environ.*, 515, 101-108, <https://doi.org/10.1016/j.scitotenv.2015.02.034>, 2015.
- Sjostedt, S. J., Slowik, J. G., Brook, J. R., Chang, Y. W., Mihele, C., Stroud, C. A., Vlasenko, A., and Abbatt, J. P. D.: Diurnally resolved particulate and VOC measurements at a rural site: indication of significant biogenic secondary organic aerosol formation, *Atmos. Chem. Phys.*, 11, 5745-5760, <https://doi.org/10.5194/acp-11-5745-2011>, 2011.
- Song, C. B., Wu, L., Xie, Y. C., He, J. J., Chen, X., Wang, T., Lin, Y. C., Jin, T. S., Wang, A. X., Liu, Y., Dai, Q. L., Liu, B. S., Wang, Y. N., and Mao, H. J.: Air pollution in China: Status and spatiotemporal variations, *Environ. Pollut.*, 227, 334-347, <https://doi.org/10.1016/j.envpol.2017.04.075>, 2017.
- Song, M., Tan, Q., Feng, M., Qu, Y., Liu, X., An, J. and Zhang, Y.: Source Apportionment and Secondary Transformation of Atmospheric Nonmethane Hydrocarbons in Chengdu, Southwest China, *J. Geophys. Res. Atmos.*, 123(17), 9741-9763, <https://doi.org/10.1029/2018JD028479>, 2018.
- Song, M. D., Li, X., Yang, S. D., Yu, X. N., Zhou, S. X., Yang, Y. M., Chen, S. Y., Dong, H. B., Liao, K. R., Chen, Q., Lu, K. D., Zhang, N. N., Cao, J. J., Zeng, L. M., and Zhang, Y. H.: Spatiotemporal variation, sources, and secondary



- transformation potential of volatile organic compounds in Xi'an China, *Atmos. Chem. Phys.*, 21, 4939-4958, <https://doi.org/10.5194/acp-21-4939-2021>, 2021.
- Song, M. D., Liu, X.G., Zhang, Y.H., Shao, M., Lu, K.D., Tan, Q.W., Feng, M. and Qu, Y.: Sources and abatement mechanisms of VOCs in southern China, *Atmos. Environ.*, 201, 28-40, <https://doi.org/10.1016/j.atmosenv.2018.12.019>, 2019a.
- Song, S. K., Shon, Z. H., Kang, Y. H., Kim, K. H., Han, S. B., Kang, M. S., Bang, J. H., and Oh, I.: Source apportionment of VOCs and their impact on air quality and health in the megacity of Seoul, *Environ. Pollut.*, 247, 763-774, <https://doi.org/10.1016/j.envpol.2019.01.102>, 2019b.
- Song, Y., Shao, M., Liu, Y., Lu, S., Kuster, W., Goldan, P., and Xie, S.: Source apportionment of ambient volatile organic compounds in Beijing, *Environ. Sci. Technol.*, 41(12), 4348-4353, <https://doi.org/10.1021/es0625982>, 2007.
- Spracklen, D. V., Jimenez, J. L., Carslaw, K. S., Worsnop, D. R., Evans, M. J., Mann, G. W., Zhang, Q., Canagaratna, M. R., Allan, J., Coe, H., McFiggans, G., Rap, A., and Forster, P.: Aerosol mass spectrometer constraint on the global secondary organic aerosol budget, *Atmos. Chem. Phys.*, 11, 12109-12136, <https://doi.org/10.5194/acp-11-12109-2011>, 2011.
- Sun, J., Shen, Z. X., Zhang, Y., Dai, W. T., He, K., Xu, H. M., Zhang, Z., Cui, L., Li, X. X., Huang, Y., and Cao, J. J.: Profiles and sources apportionment of nonmethane volatile organic compounds in winter and summer in Xian, China, based on the Hybrid Environmental Receptor Model, *Adv. Atmos. Sci.*, 38, 116-131, <https://doi.org/10.1007/s00376-020-0153-0>, 2020.
- Sun, J., Wu, F. K., Hu, B., Tang, G. Q., Zhang, J. K., and Wang, Y. S.: VOC characteristics, emissions and contributions to SOA formation during haze episodes, *Atmos. Environ.*, 141, 560-570, <https://doi.org/10.1016/j.atmosenv.2016.06.060>, 2016.
- Tan, Z., Lu, K., Jiang, M., Su, R., Dong, H., Zeng, L., Xie, S. D., Tan, Q. W., and Zhang, Y. H.: Exploring ozone pollution in Chengdu, southwestern China: A case study from radical chemistry to O₃-VOC-NO_x sensitivity, *Sci. Total Environ.*, 636, 775-786, <https://doi.org/10.1016/j.scitotenv.2018.04.286>, 2018.
- Tang, J. H., Chan, L. Y., Chan, C. Y., Li, Y. S., Chang, C. C., Wang, X. M., and Wu, D.: Implications of changing urban and rural emissions on non-methane hydrocarbons in the Pearl River Delta region of China. *Atmos. Environ.*, 42 (16), 3780-3794, <https://doi.org/10.1016/j.atmosenv.2007.12.069>, 2008.
- Toro, R., Seguel, R. J., Morales, R. G. E., and Leiva, M. A.: Ozone, nitrogen oxides, and volatile organic compounds in a central zone of Chile, *Air Qual. Atmos. Hlth.*, 8(6), 545-557, <https://doi.org/10.1007/s11869-014-0306-3>, 2015.
- US EPA: Photochemical Assessment Monitoring Stations (PAMS), available at: <http://www3.epa.gov/ttnamtl/pamsmain.html>, 1990.
- Vardoulakis, S., Solazzo, E., and Lumberras, J.: Intra-urban and street scale variability of BTEX, NO₂ and O₃ in Birmingham, UK: Implications for exposure assessment, *Atmos. Environ.*, 45(29), 5069-5078, <https://doi.org/10.1016/j.atmosenv.2011.06.038>, 2011.
- Velasco, E., Lamb, B., Westberg, H., Allwine, E., Sosa, G., Arriaga-Colina, J. L., Jobson, B. T., Alexander, M. L., Prazeller, P., Knighton, W. B., Rogers, T. M., Grutter, M., Herndon, S. C., Kolb, C. E., Zavala, M., de Foy, B., Volkamer, R., Molina, L. T., and Molina, M. J.: Distribution, magnitudes, reactivities, ratios and diurnal patterns of volatile organic compounds in the Valley of Mexico during the MCMA 2002&2003 field campaigns, *Atmos. Chem. Phys.*, 7, 329-353, <https://doi.org/10.5194/acp-7-329-2007>, 2007.
- von Schneidmesser, E., Monks, P. S., and Plass-Duelmer, C.: Global comparison of VOC and CO observations in urban areas, *Atmos. Environ.*, 44(39), 5053-5064, <https://doi.org/10.1016/j.atmosenv.2010.09.010>, 2010.
- Vo, T. D. H., Lin, C. S., Weng, C. E., Yuan, C. S., Lee, C. W., Hung, C. H., Bui, X. T., Lo, K. C., and Lin, J. X.: Vertical stratification of volatile organic compounds and their photochemical product formation potential in an industrial area, *J. Environ. Manag.*, 217, 327-336, doi:10.1016/j.jenvman.2018.03.101, 2018.
- Wang, H. L., Gao, Y. Q., Jing, S. A., Lou, S. R., Hu, Q. Y., An, J. Y., Wu, Y. H., Gao, W., Zhu, L., and Huang, C.: Characterization of volatile organic compounds (VOCs) using mobile monitoring around the industrial parks in the Yangtze River Delta region of China, *Huan jing ke xue = Huanjing kexue / [bian ji, Zhongguo ke xue yuan huan jing ke xue wei yuan hui Huan jing ke xue bian ji wei yuan hui]*, 42(3), 1298-1305, <https://doi.org/10.13227/j.hjcx.202007265>, 2021.
- Wang, M., Shao, M., Lu, S. H., Yang, Y. D., and Chen, W. T.: Evidence of coal combustion contribution to ambient VOCs during winter in Beijing, *Chin. Chem. Lett.*, 24(9), 829-832, <https://doi.org/10.1016/j.ccllet.2013.05.029>, 2013.



- Wang, P., Chen, Y., Hu, J. L., Zhang, H. L., and Ying, Q.: Source apportionment of summertime ozone in China using a source-oriented chemical transport model, *Atmos. Environ.*, 211, 79-90, <https://doi.org/10.1016/j.atmosenv.2019.05.006>, 2019a.
- Wang, P., Chen, Y., Hu, J., Zhang, H., and Ying, Q.: Attribution of tropospheric ozone to NO_x and VOC emissions: considering ozone formation in the transition regime, *Environ. Sci. Technol.*, 53, 1404-1412, <https://doi.org/10.1021/acs.est.8b05981>, 2019b.
- Wang, P., Wang, T., and Ying, Q.: Regional source apportionment of summertime ozone and its precursors in the megacities of Beijing and Shanghai using a source-oriented chemical transport model, *Atmos. Environ.*, 224, 117337, <https://doi.org/10.1016/j.atmosenv.2020.117337>, 2020.
- Wang, Q., Liu, M., Yu, Y. P., and Li, Y.: Characterization and source apportionment of PM_{2.5}-bound polycyclic aromatic hydrocarbons from Shanghai city, China, *Environ. Pollu.*, 218, 118-128, <https://doi.org/10.1016/j.envpol.2016.08.037>, 2016.
- Wang, R., Xu, X. B., Jia, S. H., Ma, R. S., Ran, L., Deng, Z. Z., Lin, W. L., Wang, Y., and Ma, Z. Q.: Lower tropospheric distributions of O₃ and aerosol over Raoyang, a rural site in the North China Plain, *Atmos. Chem. Phys.*, 17, 3891-3903, <https://doi.org/10.5194/acp-17-3891-2017>, 2017.
- Warneke, C., de Gouw, J. A., Holloway, J. S., Peischl, J., Ryerson, T. B., Atlas, E., Blake, D., Trainer, M., and Parrish, D. D.: Multiyear trends in volatile organic compounds in Los Angeles, California: five decades of decreasing emissions, *J. Geophys. Res. Atmos.*, 117(17), 1-10, <https://doi.org/10.1029/2012JD017899>, 2012.
- Wei, X. Y., Liu, M., Yang, J., Du, W. N., Sun, X., Huang, Y. P., Zhang, X., Khalil, S. K., Luo, D. M., and Zhou, Y. D.: Characterization of PM_{2.5}-bound PAHs and carbonaceous aerosols during three-month severe haze episode in Shanghai, China: Chemical composition, source apportionment and long-range transportation, *Atmos. Environ.*, 203, 1-9, <https://doi.org/10.1016/j.atmosenv.2019.01.046>, 2019.
- Wongphatarakul, V., Fridelander, S. K., and Pinto, J. P.: A comparative study of PM_{2.5} ambient aerosol chemical databases, *Environ. Sci. Technol.*, 32, 3926-3934, [https://doi.org/10.1016/S0021-8502\(98\)00164-5](https://doi.org/10.1016/S0021-8502(98)00164-5), 1998.
- Wu, R. G., Li, J., Hao, Y. F., Li, Y. Q., Zeng, L. M., and Xie, S. D.: Evolution process and sources of ambient volatile organic compounds during a severe haze event in Beijing, China, *Sci. Total Environ.*, 560-561, 62-72, <https://doi.org/10.1016/j.scitotenv.2016.04.030>, 2016.
- Wu, R. R., Li, J., Hao, Y. F., Li, Y. Q., Zeng, L. M., and Xie, S. D.: Evolution process and sources of ambient volatile organic compounds during a severe haze event in Beijing, China, *Sci. Total Environ.*, 560-561, 62-72, <https://doi.org/10.1016/j.scitotenv.2016.04.030>, 2016.
- Xie, Y. L., and Berkowitz, C. M.: The use of conditional probability functions and potential source contribution functions to identify source regions and advection pathways of hydrocarbon emissions in Houston, Texas, *Atmos. Environ.*, 41, 5831-5847, <https://doi.org/10.1016/j.atmosenv.2007.03.049>, 2007.
- Xu, J. M., Tie, X. X., Gao, W., Lin, Y. F., Fu, and Fu, Q. Y.: Measurement and model analyses of the ozone variation during 2006 to 2015 and its response to emission change in megacity Shanghai, China, *Atmos. Chem. Phys.* 19, 9017-9035, <https://doi.org/10.5194/acp-19-9017-2019>, 2019.
- Xue, L. K., Wang, T. J., Gao, J. A., Ding, A. J., Zhou, X. H., Blake, D. R., Wang, X. F., Saunders, S., Fan, S. J., Zuo, H. C., Zhang, Q. Z., and Wang, W. X.: Ground-level ozone in four Chinese cities: precursors, regional transport and heterogeneous processes, *Atmos. Chem. Phys.*, 14(23), 13175-13188, <https://doi.org/10.5194/acp-14-13175-2014>, 2014.
- Yan, Y. L., Peng, L., Li, R. M., Li, Y. H., Li, L. J., and Bai, H. L.: Concentration, ozone formation potential and source analysis of volatile organic compounds (VOCs) in a thermal power station centralized area: A study in Shuozhou, China, *Environ. Pollut.*, 223, 295-304, <https://doi.org/10.1016/j.envpol.2017.01.026>, 2017.
- Yao, Z., Wu, B., Shen, X., Cao, X., Jiang, X., Ye, Y., and He, K.: On-road emission characteristics of VOCs from rural vehicles and their ozone formation potential in Beijing, China, *Atmos. Environ.*, 105, 91-96, <https://doi.org/10.1016/j.atmosenv.2015.01.054>, 2015.
- Yang, H., Zhu, B., Gao, J., Li, Y., and Xia, L.: Source apportionment of VOCs in the northern suburb of Nanjing in summer, *Environ. Sci.*, 34(12), 4519-4528, 2013.
- Yang, Y. R., Liu, X. G., Qu, Y., An, J. L., Jiang, R., and Zhang, Y. H.: Characteristics and formation mechanism of continuous hazes in China: a case study during the autumn of 2014 in the North China Plain, *Atmos. Chem. Phys.*, 15, 8165-8178, <https://doi.org/10.5194/acpd-15-10987-2015>, 2015.



- Yu, S. J., Su, F. C., Yin, S. S., Wang, S. B., Xu, R. X., He, B., Fan, X. G., Yuan, M. H., and Zhang, R. Q.: Characterization of ambient volatile organic compounds, source apportionment, and the ozone-NO_x-VOC sensitivities in a heavily polluted megacity of central China: Effect of sporting events and the emission reductions, *Atmos. Chem. Phys.*, 293, 1-61, <https://doi.org/10.5194/acp-21-15239-2021>, 2021.
- Yuan, B., Hu, W. W., Shao, M., Wang, M., Chen, W. T., Lu, S. H., Zeng, L. M., and Hu, M.: VOCs emissions, evolutions and contributions to SOA formation at a receptor site in eastern China, *Atmos. Chem. Phys.*, 13(17), 8815-8832, <https://doi.org/10.5194/acp-13-8815-2013>, 2013.
- Yuan, B., Shao, M., Lu, S., and Wang, B.: Source profiles of volatile organic compounds associated with solvent use in Beijing, China, *Atmos. Environ.*, 44, 1919-1926, <https://doi.org/10.1016/j.atmosenv.2010.02.014>, 2010.
- Yuan, B., Hu, W. W., Shao, M., Wang, M., Chen, W. T., Lu, S. H., Zeng, L. M., and Hu, M.: VOCs emissions, evolutions and contributions to SOA formation at a receptor site in eastern China, *Atmos. Chem. Phys.*, 13(17), 8815-8832, <https://doi.org/10.5194/acp-13-8815-2013>, 2013.
- Zhang, D., He, B., Yuan, M. H., Yu, S. J., Yin, S. S., and Zhang, R. Q.: Characteristics, sources and health risks assessment of VOCs in Zhengzhou, China during the haze pollution season, *J. Environ. Sci.*, 108, 44-57, <https://doi.org/10.1016/j.jes.2021.01.035>, 2021.
- Zhang, F., Shang, X. N., Chen, H., Xie, G. Z., Fu, Y., Wu, D., Sun, W. W., Liu, P. F., Wang, G. H., and Chen, J. M.: Significant impact of coal combustion on VOCs emissions in winter in a North China rural site, *Sci. Total Environ.*, 720, 137617, 1-11, <https://doi.org/10.1016/j.scitotenv.2020.137617>, 2020b.
- Zhang, G., Wang, N., Jiang, X., and Zhao, Y.: Characterization of ambient volatile organic compounds (VOCs) in the area adjacent to a petroleum refinery in Jinan, China, *Aerosol Air Qual. Res.*, 17(4), 944-950, <https://doi.org/10.4209/aaqr.2016.07.0303>, 2017.
- Zhang, J. Z., Wang, T. J., Chameides, W. L., Cardelino, C., Joey, Y. W., Blake, D. R., Ding, A. J., and So, K. L.: Ozone production and hydrocarbon reactivity in HongKong, Southern China, *Atmos. Chem. Phys.*, 7, 557-573, <https://doi.org/10.5194/acp-7-557-2007>, 2007.
- Zhang, K., Li, L., Huang, L., Wang, Y. J., Huo, J. T., Duan, Y. S., Wang, Y. H., and Fu, Q. Y.: The impact of volatile organic compounds on ozone formation in the suburban area of Shanghai, *Atmos. Environ.*, 232(137617), 1-11, <https://doi.org/10.1016/j.atmosenv.2020.117511>, 2020a.
- Zhang, Y., Wang, X., Zhang, Z., Lu, S., Shao, M., Lee, F. S. C., and Yu, J.: Species profiles and normalized reactivity of volatile organic compounds from gasoline evaporation in China, *Atmos. Environ.*, 79, 110-118, <https://doi.org/10.1016/j.atmosenv.2013.06.029>, 2013.
- Zhang, Y. C., Li R., Fu H. B., Zhou D., and Chen J. M.: Observation and analysis of atmospheric volatile organic compounds in a typical petrochemical area in Yangtze River Delta, China, *J. Environ. Sci.*, 71, 233-248, <https://doi.org/CNKI:SUN:HJKB.0.2018-09-022>, 2018.
- Zheng, J., Yu, Y., Mo, Z., Zhang, Z., Wang, X., Yin, S., Peng, K., Yang, Y., Feng, X., and Cai, H.: Industrial sector-based volatile organic compound (VOC) source profiles measured in manufacturing facilities in the Pearl River Delta, China, *Sci. Total Environ.*, 456, 127-136, <https://doi.org/10.1016/j.scitotenv.2013.03.055>, 2013.
- Zheng, J. Y., Zhong, L. J., Wang, T., Louie, P. K. K., and Li, Z. C.: Ground-level ozone in the Pearl River Delta region: analysis of data from a recently established regional air quality monitoring network, *Atmos. Environ.*, 44, 814-823, <https://doi.org/10.1016/j.atmosenv.2009.11.032>, 2010.
- Zheng, H., Kong, S. F., Xing, X. L., Mao, Y., Hu, Y. P., Ding, Y., Li, G., Liu, D. T., Li, S. L., and Qi, S. H.: Monitoring of volatile organic compounds (VOCs) from an oil and gas station in northwest China for 1 year, *Atmos. Chem. Phys.*, 18(7), 4567-4595, <https://doi.org/10.5194/acp-2017-828>, 2018.
- Zheng, H., Kong, S. F., Yan, Y. Y., Chen, N., Yao, L. Q., Liu, X., Wu, F. Q., Cheng, Y., Niu, Z. Z., Zheng, S. R., Zeng, X., Yan, Q., Wu, J., Zheng, M. M., Liu, D. T., Zhao, D. L., and Qi, S. H.: Compositions, sources and health risks of ambient volatile organic compounds (VOCs) at a petrochemical industrial park along the Yangtze River, *Sci. Total. Environ.*, 73, 135505, 1-12, <https://doi.org/10.1016/j.scitotenv.2019.135505>, 2020.
- Zhu, H. L., Wang, H. L., Jing, S. G., Wang, Y. F., Cheng, T. T., Tao, S. K., Lou, S. R., Qiao, L. P., Li, L., and Chen, J. M.: Characteristics and sources of atmospheric volatile organic compounds (VOCs) along the mid-lower Yangtze River in China, *Atmos. Environ.*, 190(7), 232-240, <https://doi.org/10.1016/j.atmosenv.2018.07.026>, 2018.
- Zhu, Y., Yang, L., Chen, J., Wang, X., Xue, L., Sui, X., Wen, L., Xu, C., Yao, L., Zhang, J., Shao, M., Lu, S., and Wang, W.:



- Characteristics of ambient volatile organic compounds and the influence of biomass burning at a rural site in Northern China during summer 2013, *Atmospheric Environment*, 124, 156-165, <https://doi.org/10.1016/j.atmosenv.2015.08.097>, 2016.
- Zhu, Y. H., Yang, L. X., Kawamura, K., Chen, J. M., Ono, K. R., Wang, X. F., Xue, L. K., and Wang, W. X.: Contribution and source identification of biogenic and anthropogenic hydrocarbons to secondary organic aerosols at Mt. Tai in 2014, *Environ. Pollut.*, 220, 863-872, <https://doi.org/10.1016/j.envpol.2016.10.070>, 2017.
- Zou, B. B., Huang, X. F., Zhang, B., Dai, J., Zeng, L. W., Feng, N., and He, L. Y.: Source apportionment of PM_{2.5} pollution in an industrial city in southern China, *Atmos. Pollut. Re.*, 8(6), 1193-1202, <https://doi.org/10.1016/j.apr.2017.05.001>, 2017.

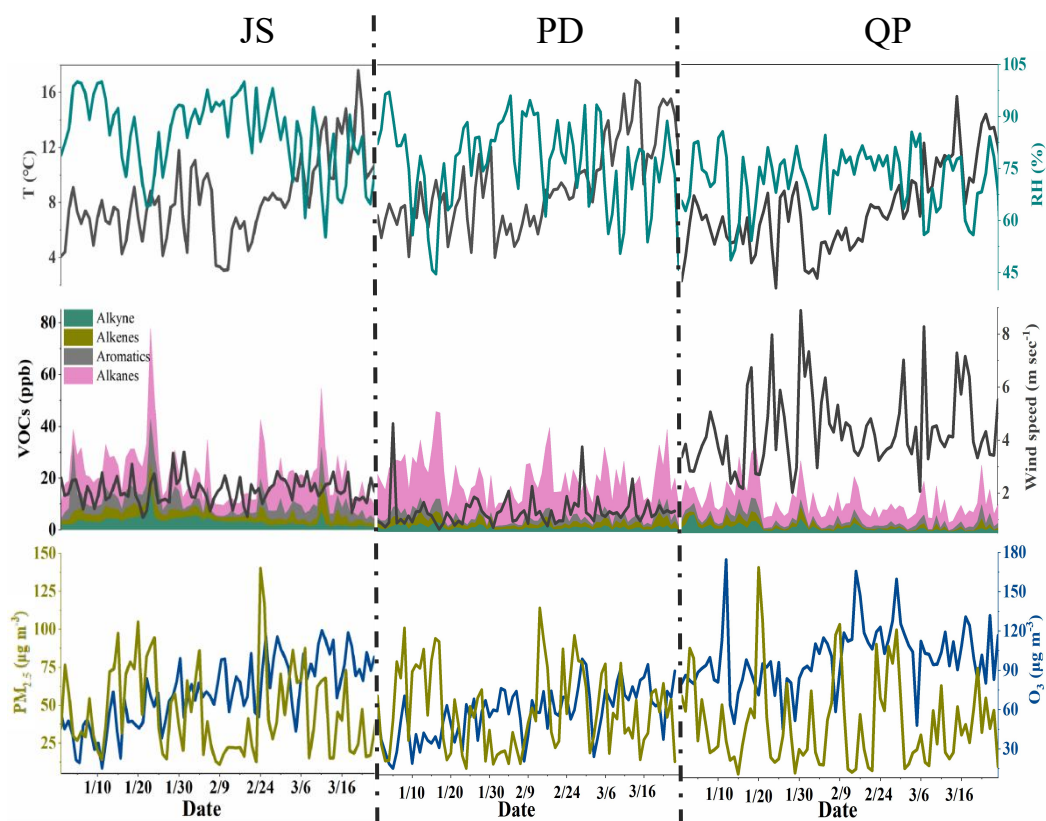


Figure 1: Time series of temperature (T), relative humidity (RH), wind speed, VOC categories, PM_{2.5} and O₃ at the (a) JS, (b) PD and (c) QP sites.

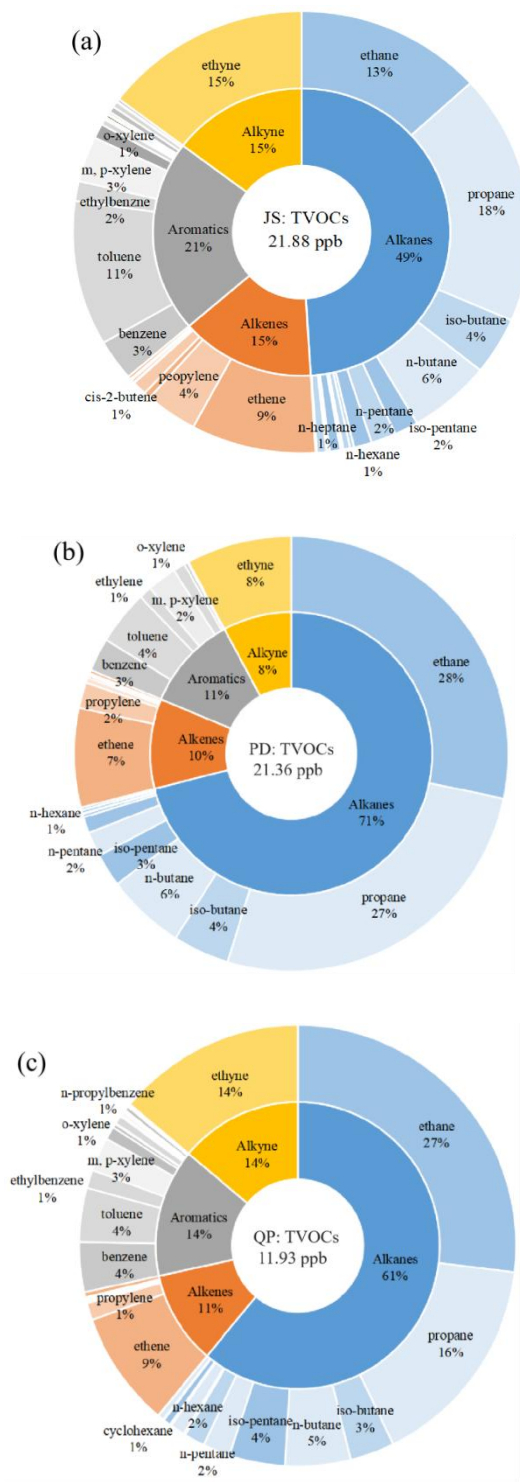


Figure 2: Contributions of the VOC categories (43 species) at the (a) JS, (b) PD and (c) QP sites (the contributions > 1 % were marked).

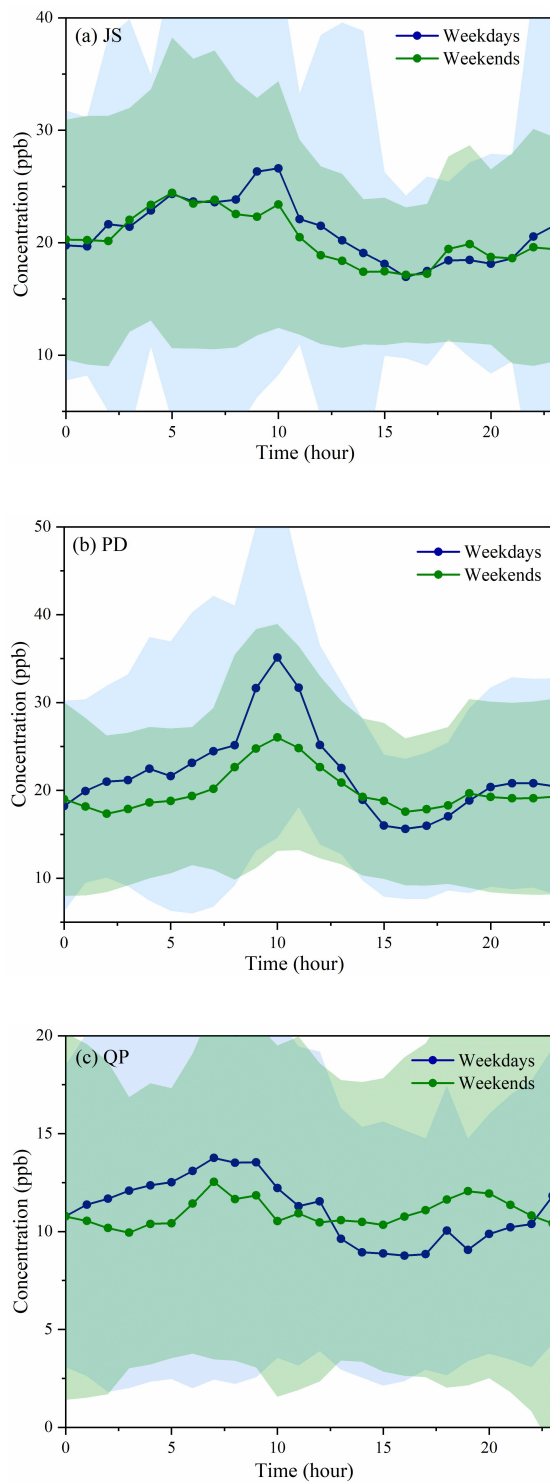


Figure 3: Weekend effects of the TVOC concentrations at the sampling sites.

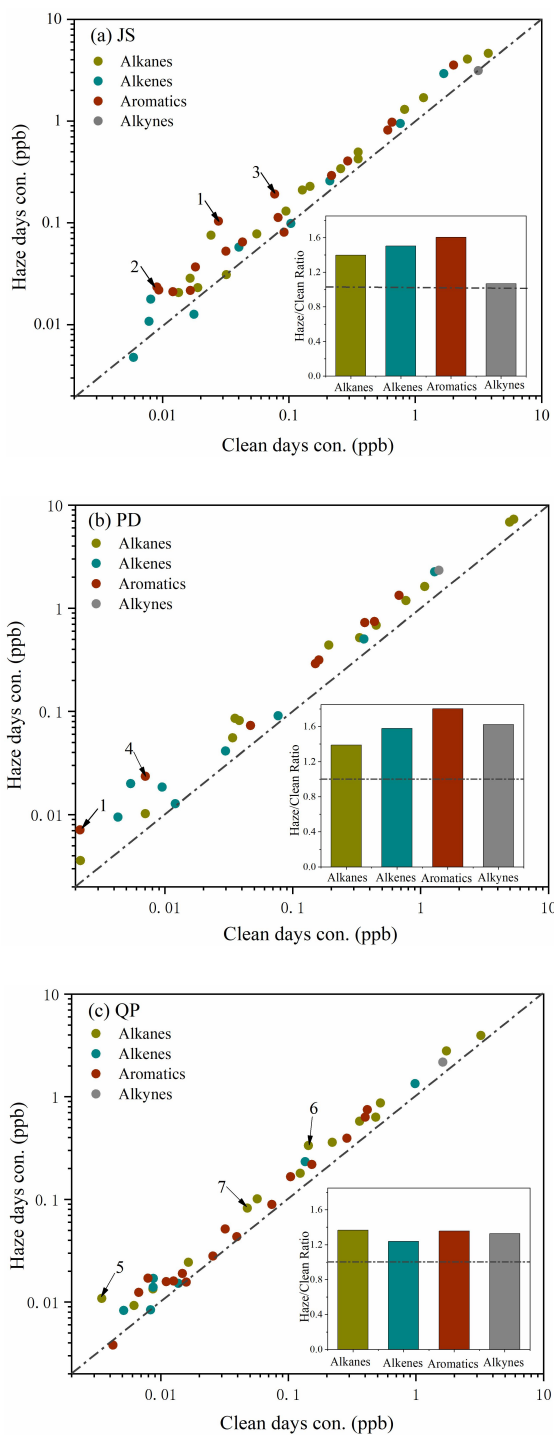


Figure 4: Differences in VOC concentrations between the clean and haze days at the (a) JS, (b) PD and (c) QP sites. 1: 1, 2, 4-trimethylbenzene; 2: *p*-ethylbenzene; 3: *m*-dimethylbenzene; 4: *m*-ethylbenzene; 5: 2, 2, 4-trimethylpentane; 6: *n*-hexane; 7: *h*-heptane.

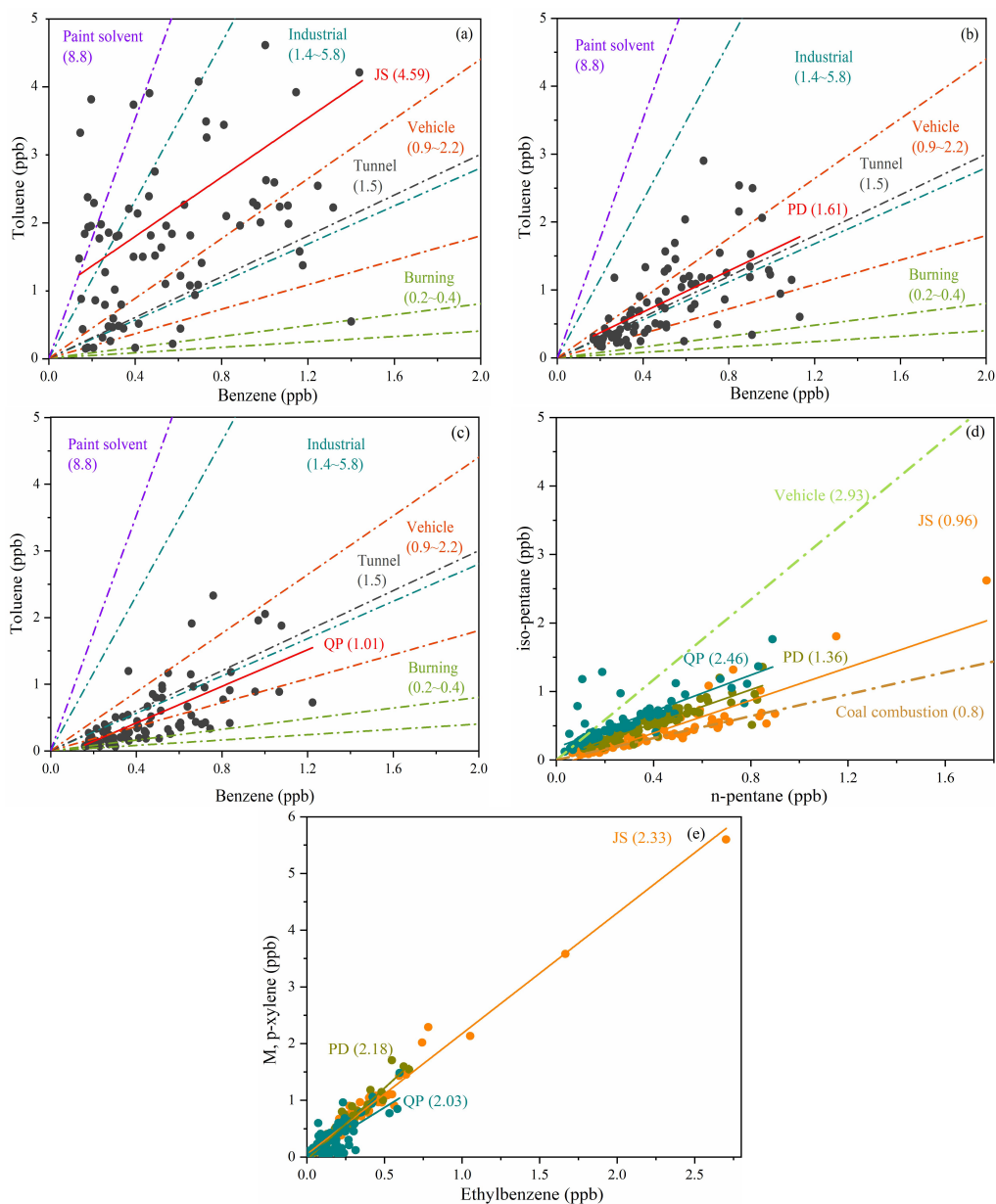
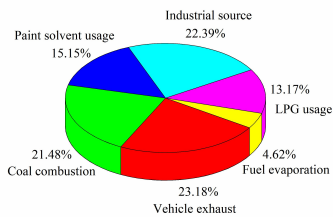
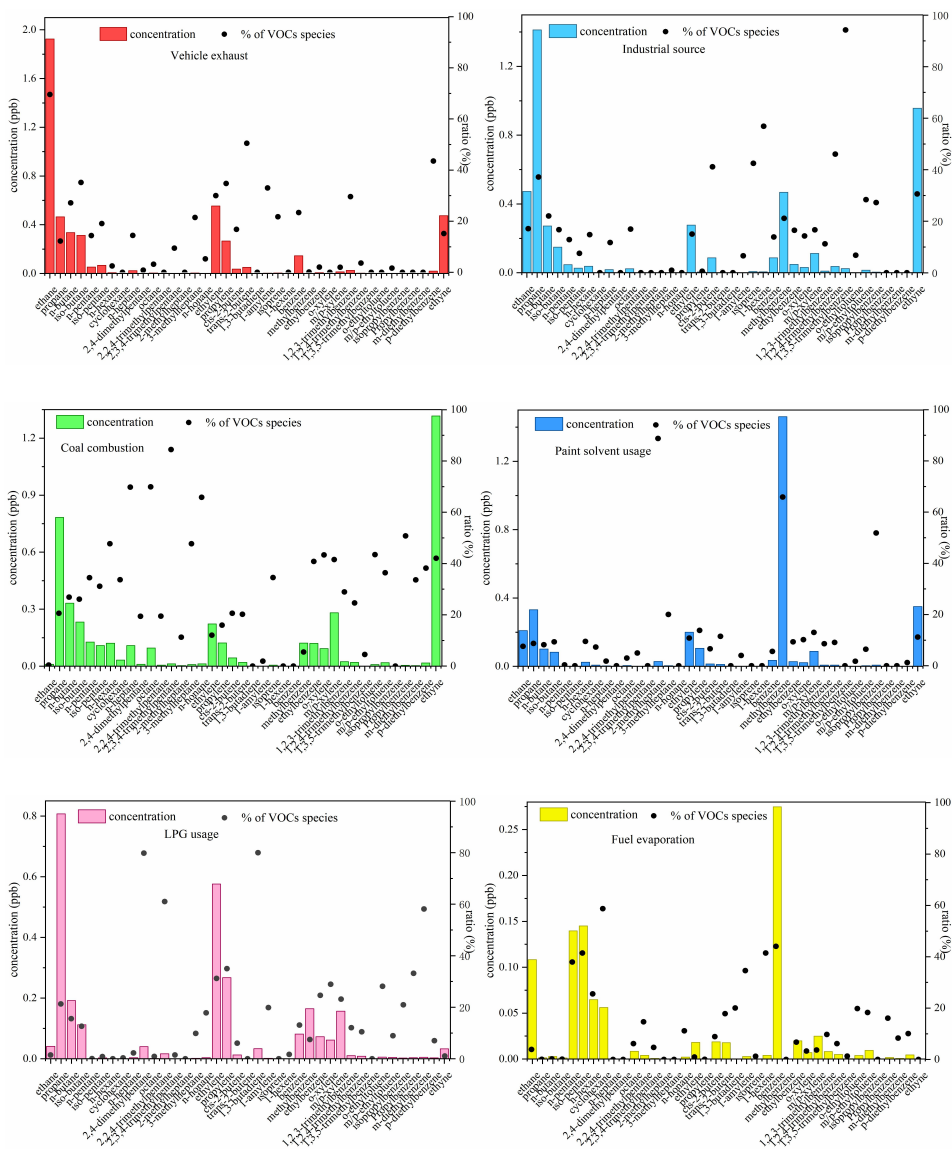
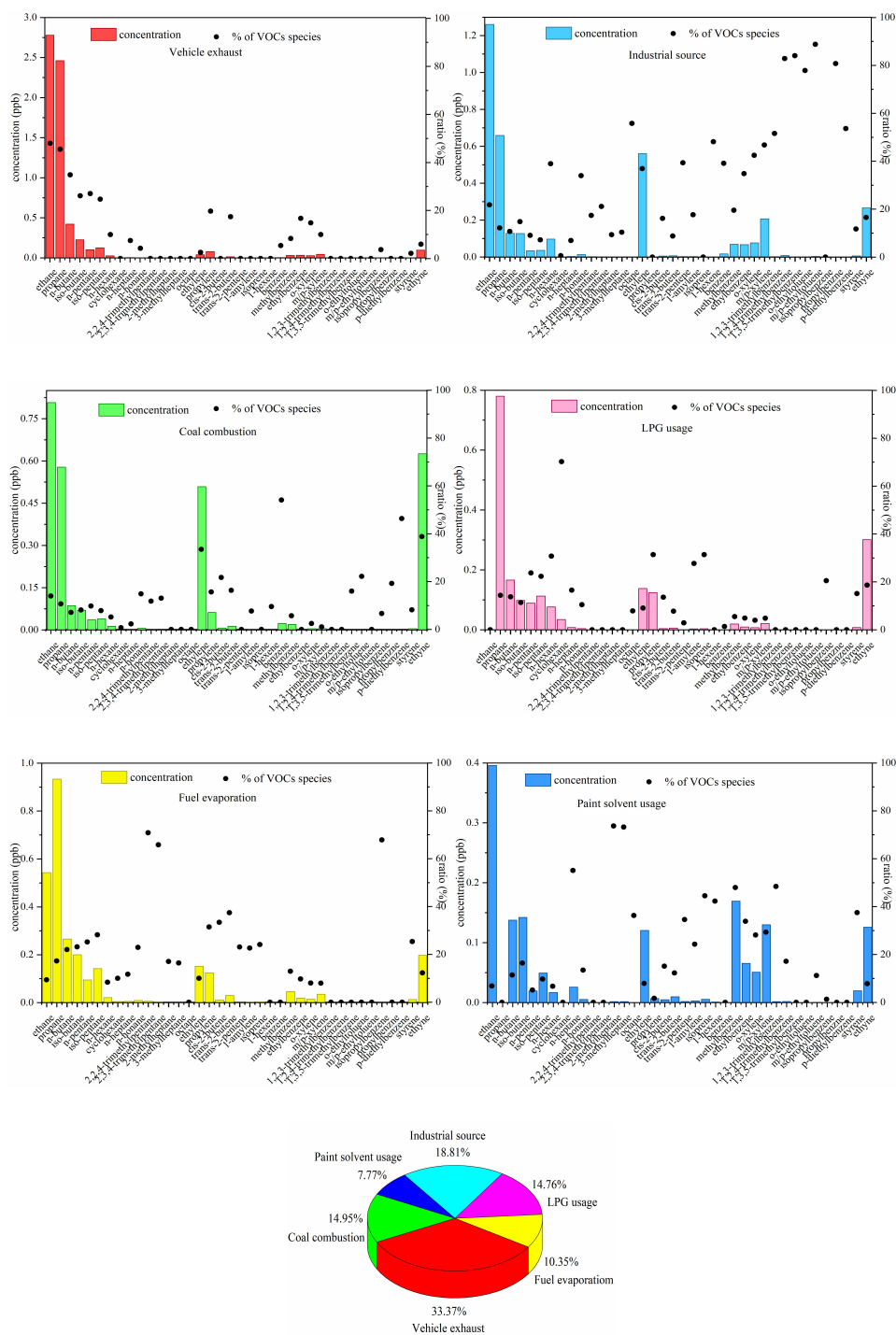


Figure 5: Specific ratios of the target VOC species for the source identification. The linear correlations between toluene and benzene at the (a) JS, (b) PD and (c) QP sites, and (d) *m*, *p*-xylene and ethylbenzene and (e) *iso*-pentane and *n*-pentane at JS (orange), PD (yellow) and QP (blue).

a. JS



b. PD



c. QP

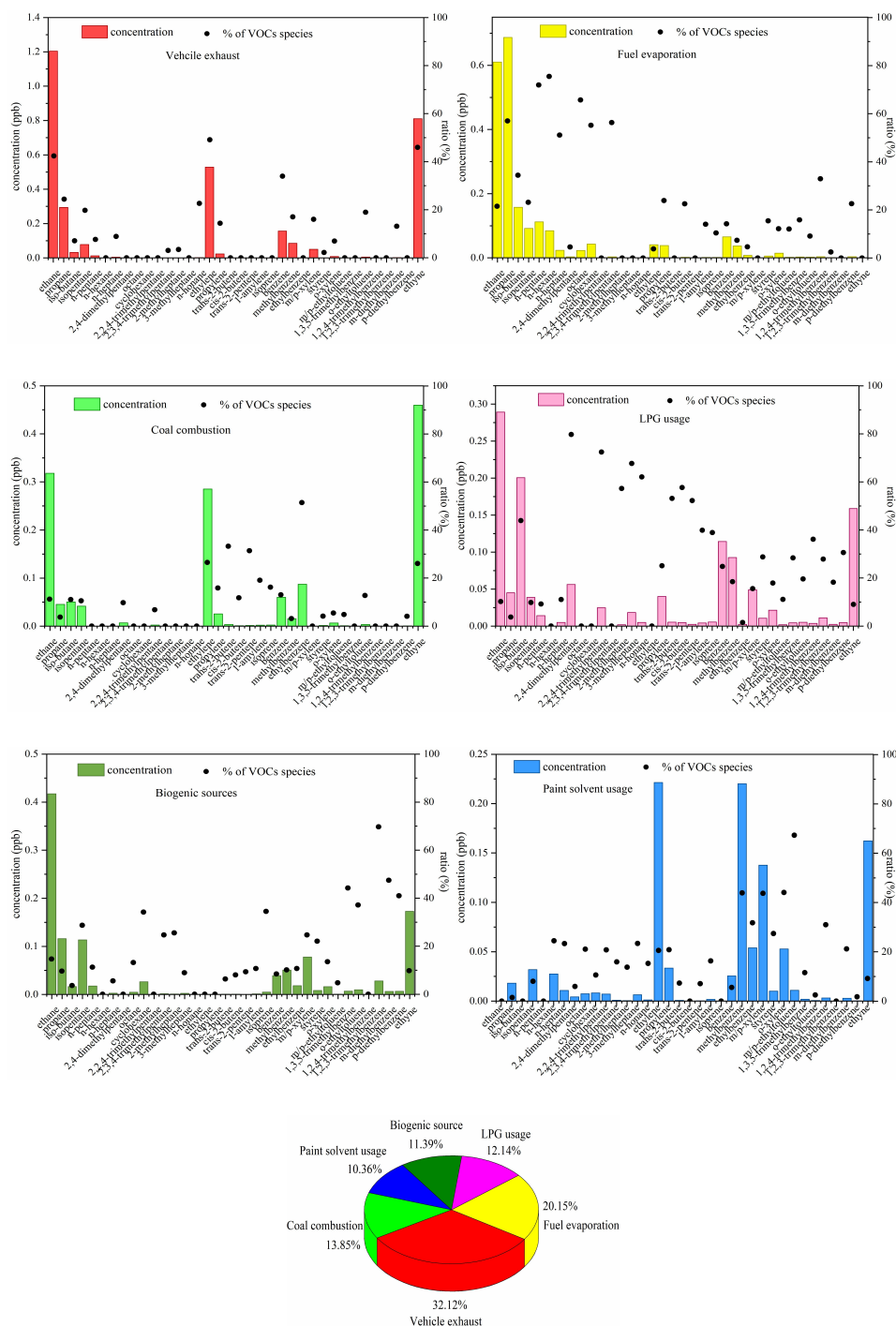


Figure 6: Sources profiles and contributions of VOCs at the (a) JS, (b) PD and (c) QP sites.

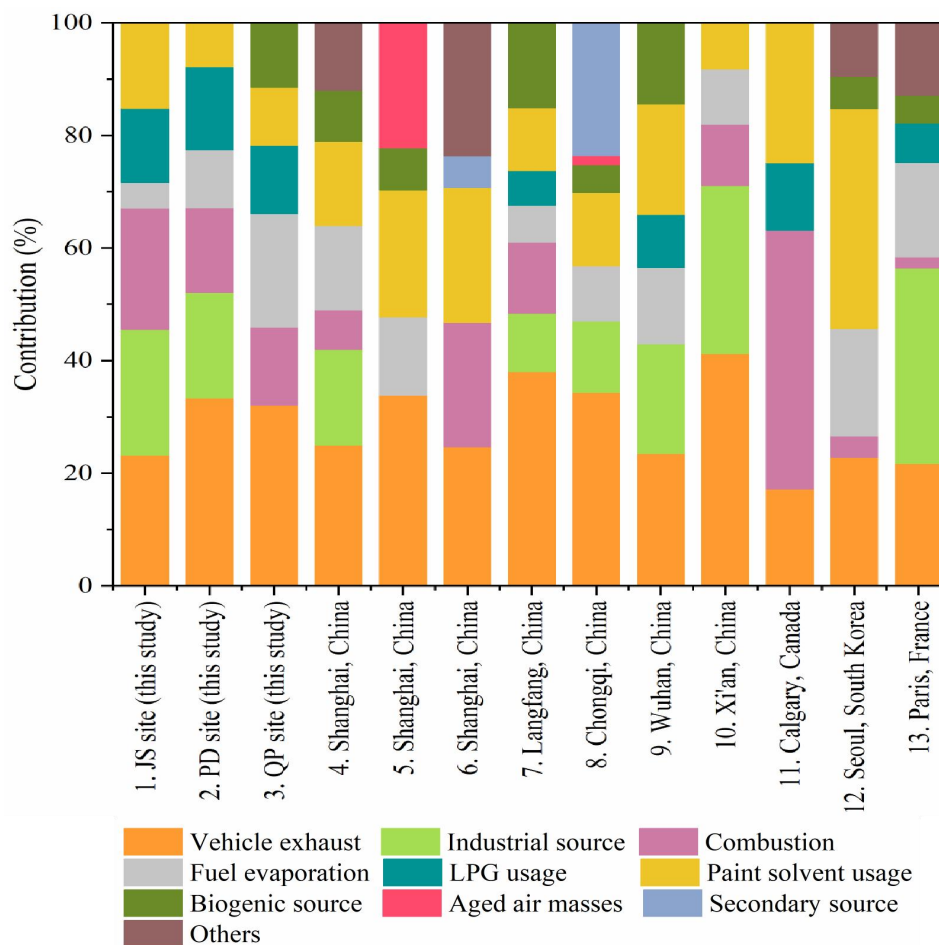
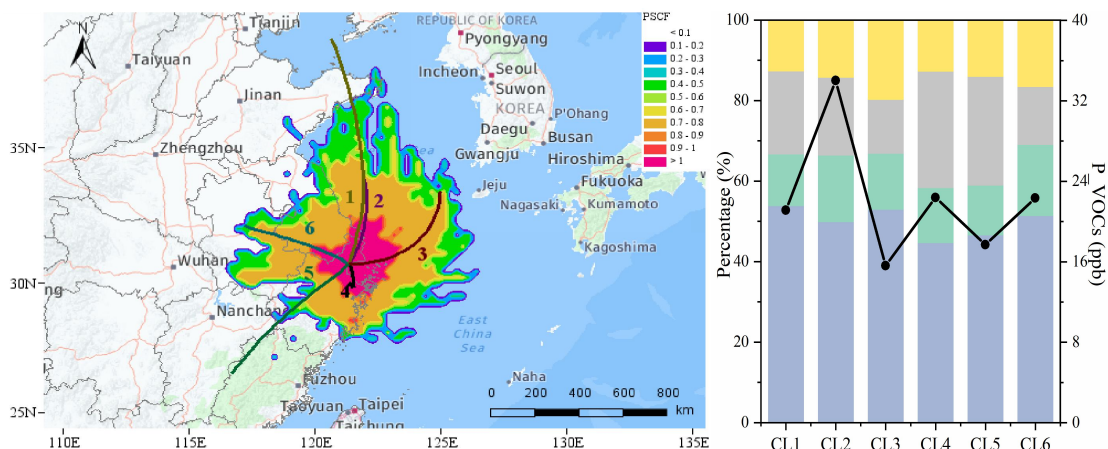


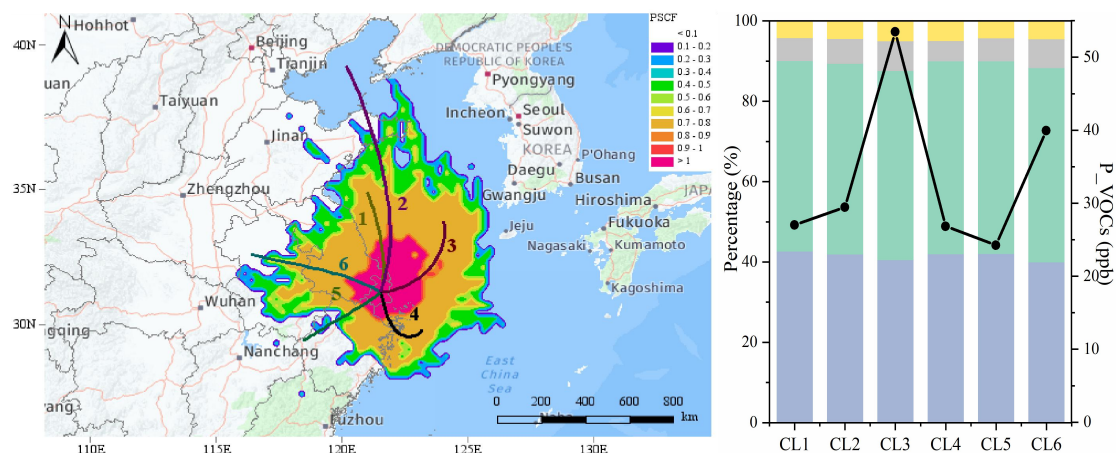
Figure 7: Primary emissions of the observed atmospheric VOCs of this study, and those measured at different locations or during different periods: 1, 2, 3. Shanghai, China (this study); 4. Shanghai, China (Cai et al., 2010b); 5. Shanghai, China (Liu et al., 2019); 6. Shanghai, China (Liu et al., 2021); 7. Langfang, China (Song et al., 2019a); 8. Chongqi, China (Li et al., 2018); 9. Wuhan, China (Hui et al., 2018); 10. Xi'an, China (Song et al., 2021); 11. Calgary, Canada (Bari and Kindzierski, 2018); 12. Seoul, South Korea (Song et al., 2019b); 13. Paris, France (Gaimoz et al., 2011)



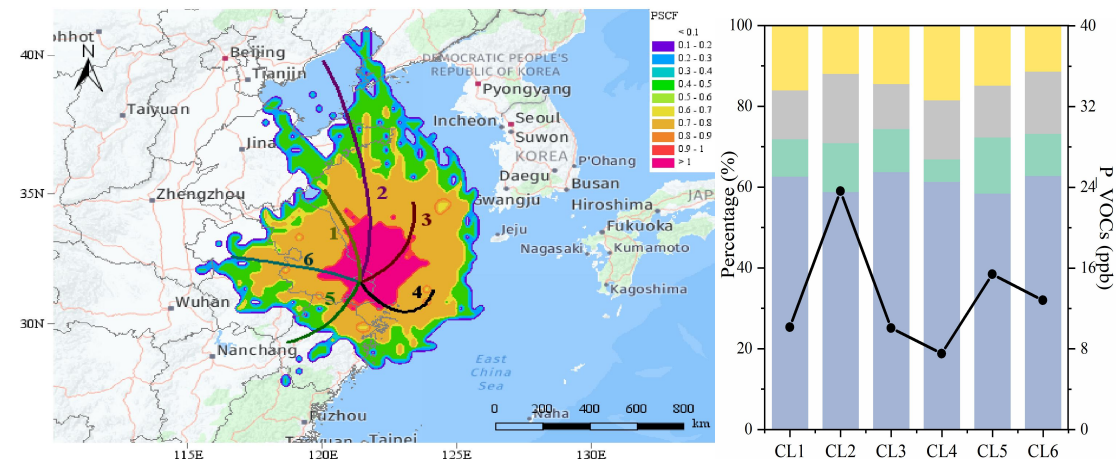
a. JS



b. PD



c. QP



Alkanes Alkenes Aromatics Alkyne P_TVOCs

Figure 8: Backward trajectory cluster analysis (24 h) and PSCF analysis at the JS, PD and QP sites.

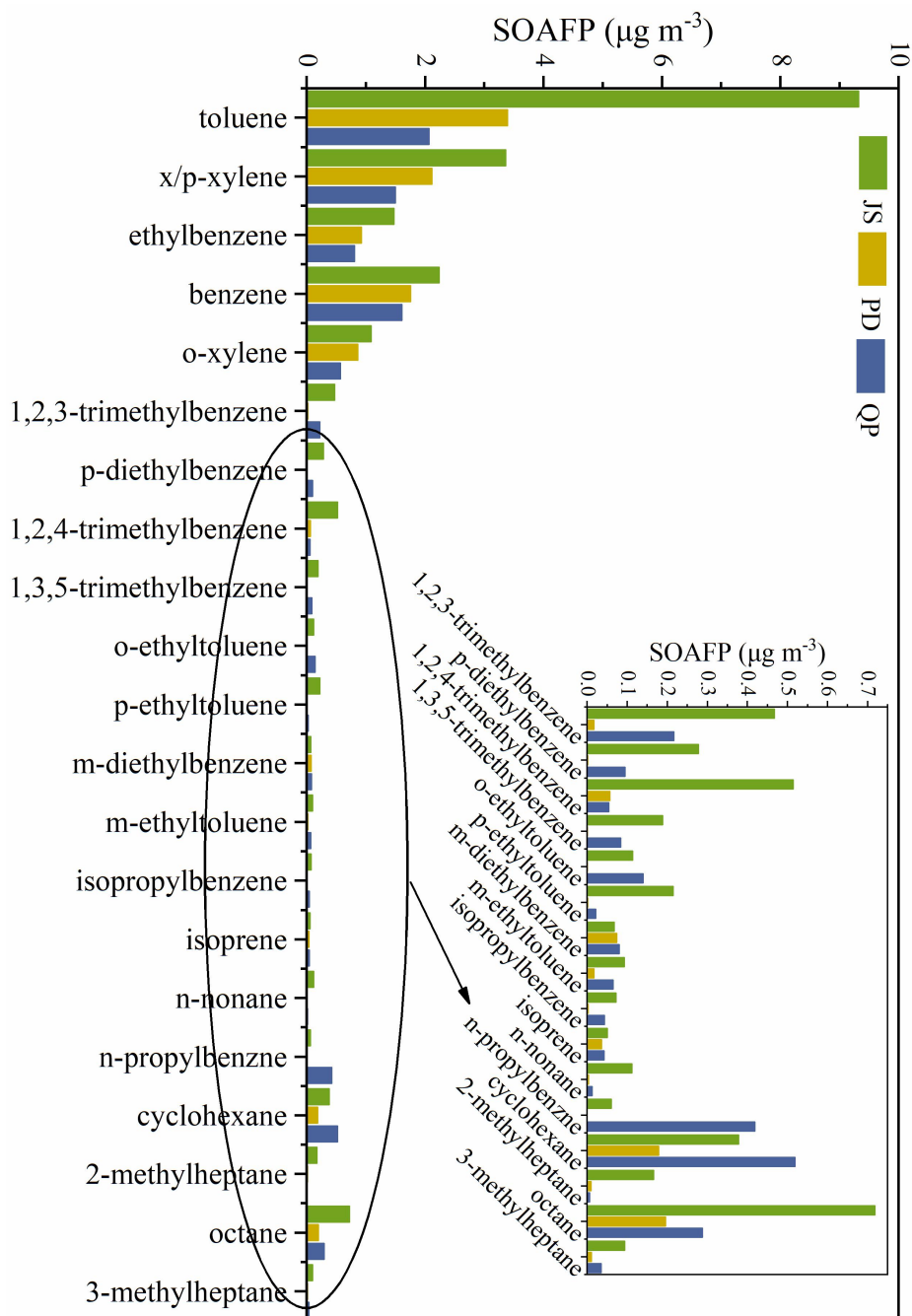


Figure 9: The SOAFP analysis of different VOC species at the JS, PD and QP sites.

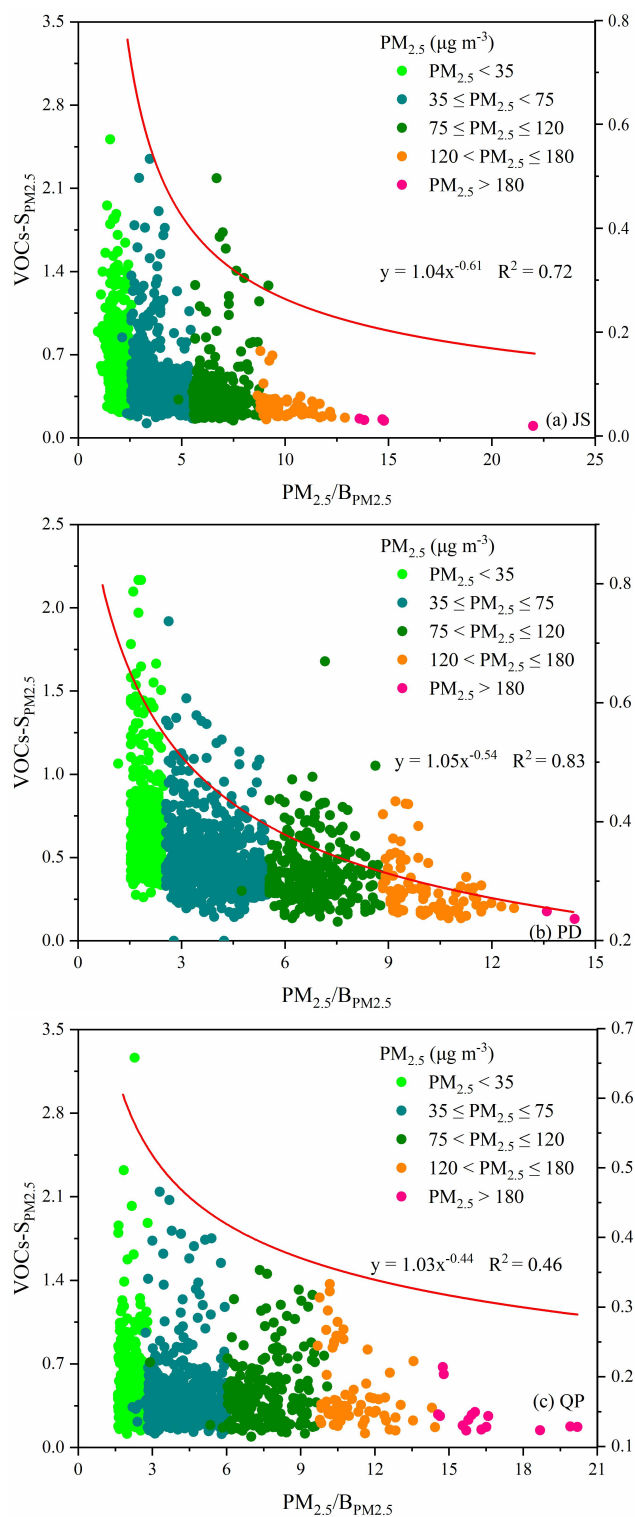


Figure 10: The variations of $VOCs-S_{PM2.5}$ at the different level of $PM_{2.5}$ at the JS, PD and QP sites.

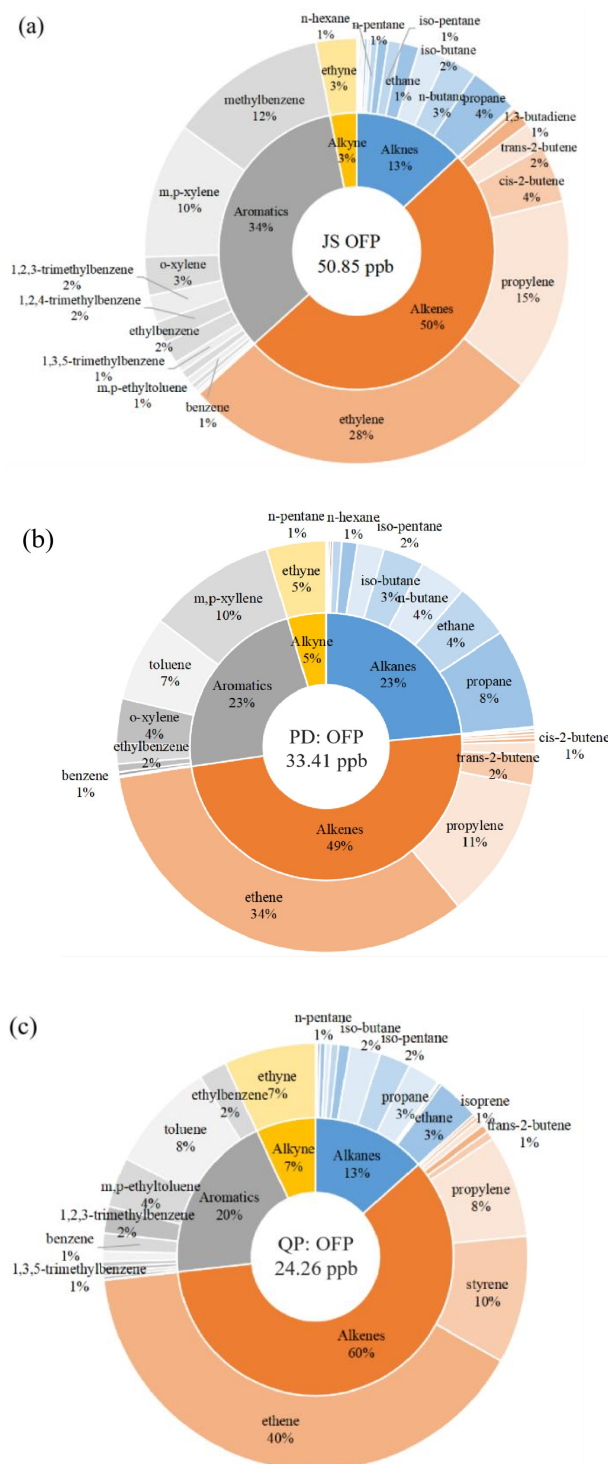


Figure 11: Contributions of VOCs to OFP at the (a) JS, (b) PD and (c) QP sites (the contributions > 1 % were marked).

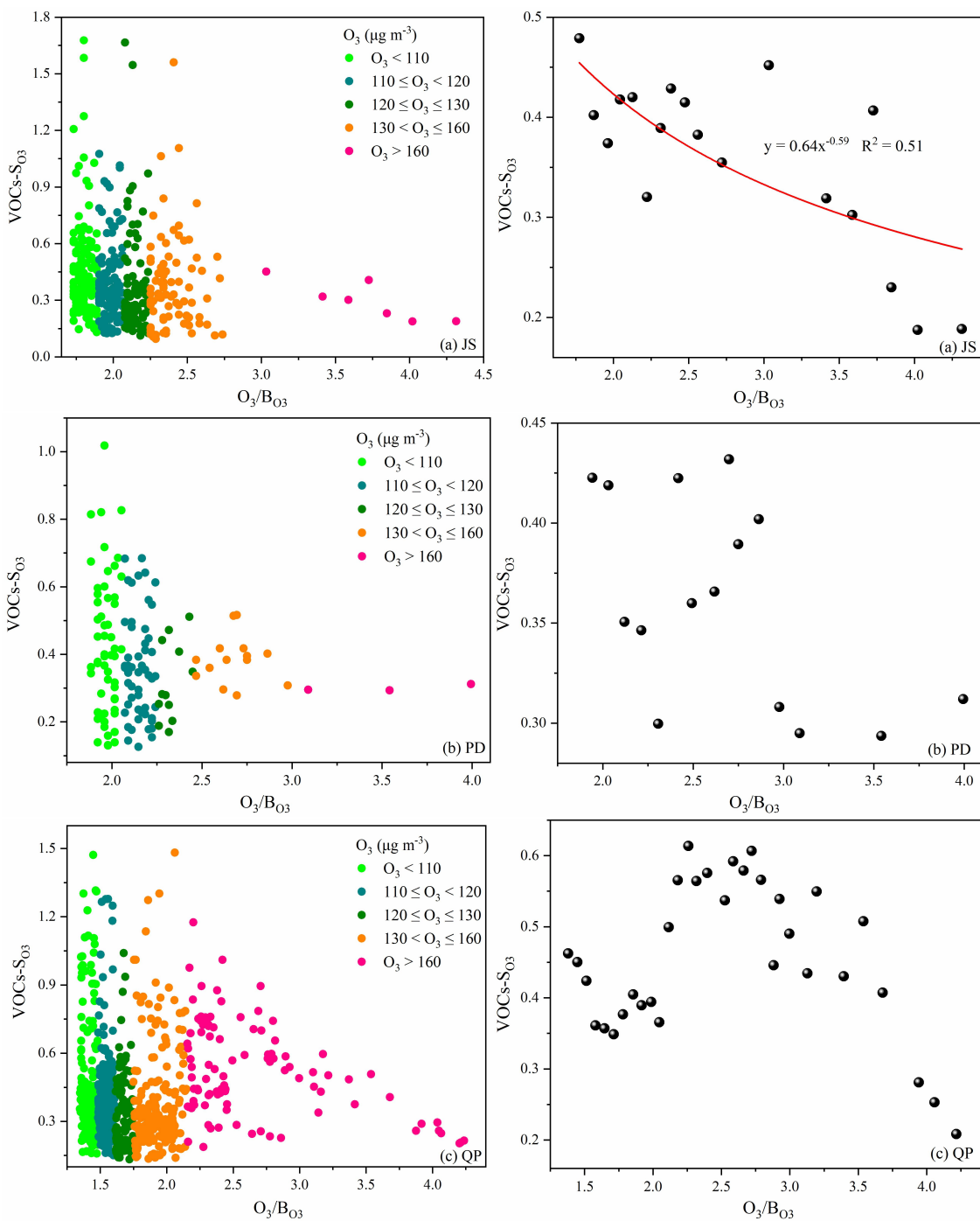


Figure 12: The variations of VOCs-S₀₃ at the different level of O₃ at the JS, PD and QP sites.



Table 1: Air mass cluster trajectories at the JS, PD and QP sites.

Site	Cluster	Ratio (%)	P_Ratio (%)	P_TVOCs (ppb)
JS	1	16.67	28.04	21.13
	2	29.07	18.03	34.03
	3	19.46	16.62	15.62
	4	12.26	12.75	22.40
	5	5.92	16.62	17.70
	6	16.62	5.93	22.34
PD	1	18.04	33.13	27.03
	2	17.80	10.42	29.45
	3	34.19	21.59	53.48
	4	8.57	15.28	26.85
	5	10.84	8.53	24.25
	6	10.56	11.04	39.95
QP	1	14.20	18.47	10.15
	2	17.57	13.50	23.63
	3	31.87	27.81	10.07
	4	15.20	16.79	7.53
	5	8.71	14.52	15.39
	6	12.45	8.91	12.81